Exome sequencing of healthy phenotypic extremes links *TROVE2* to emotional memory and PTSD

Angela Heck[1,2,3], Annette Milnik[1,2,3], Vanja Vukojevic[1,2,4], Jana Petrovska[1,2], Tobias Egli[1,2], Jochen Singer[5,6], Pablo Escobar[6,7,8], Thierry Sengstag[6,7,8], David Coynel[2,9], Virginie Freytag[1,2], Matthias Fastenrath[2,9], Philippe Demougin[1,2,4], Eva Loos[2,9], Francina Hartmann[1,2], Nathalie Schicktanz[2,9], Bernardo Delarue Bizzini[1,2,4], Christian Vogler[1,2,3], Iris-Tatjana Kolassa[10], Sarah Wilker[10], Thomas Elbert[11], Torsten Schwede[6,7,8], Christian Beisel[5], Niko Beerenwinkel[5,6], Dominique J.-F. de Quervain[2,3,9,+], Andreas Papassotiropoulos[1,2,3,4,*,+]

[1]Division of Molecular Neuroscience, Department of Psychology, University of Basel, CH-4055 Basel, Switzerland
[2]Transfaculty Research Platform Molecular and Cognitive Neurosciences, University of Basel, CH-4055 Basel, Switzerland
[3]Psychiatric University Clinics, University of Basel, CH-4055 Basel, Switzerland
[4]Department Biozentrum, Life Sciences Training Facility, University of Basel, CH-4056 Basel, Switzerland
[5]Department of Biosystems Science and Engineering, ETH Zurich, CH-4058 Basel, Switzerland
[6]SIB Swiss Institute of Bioinformatics, CH-4056 Basel, Switzerland
[7]Department Biozentrum, University of Basel, CH-4056 Basel, Switzerland
[8]sciCORE Center for Scientific Computing, University of Basel, CH-4056 Basel, Switzerland
[9]Division of Cognitive Neuroscience, Department of Psychology, University of Basel, CH-4055 Basel, Switzerland
[10]Clinical & Biological Psychology, Institute of Psychology & Education, Ulm University, D-89069 Ulm, Germany
[11]Department of Psychology, University of Konstanz, D-78457 Konstanz, Germany

*Correspondence to: andreas.papas@unibas.ch or angela.heck@unibas.ch
+ Co-senior author

ABSTRACT

Many mental disorders represent the extremes of normal distributions of traits related to multiple cognitive and emotional dimensions. By performing whole-exome sequencing in healthy young subjects with extremely high versus extremely low aversive memory performance we identified *TROVE2* as a gene implicated in emotional memory in health and disease. *TROVE2* encodes Ro60, a broadly-expressed RNA-binding protein centrally implicated in the regulation of inflammatory gene expression and autoimmunity. A regulatory *TROVE2* variant was linked to higher emotional memory capacity and higher emotional memory-related brain activation in healthy subjects. In addition, *TROVE2* was associated with traumatic memory and the frequency of posttraumatic stress disorder in genocide survivors.

Introduction

Enhanced memory for emotional events, a common observation in animals and humans, is an evolutionary important trait, because it helps remembering both dangerous and favorable situations [1]. On the other hand, strong sensory and emotional memories of various life-threatening and aversive experiences may contribute to the development and symptoms of posttraumatic stress disorder (PTSD) [2,3], especially when such memories loose their association to the original contextual system [4,5]. In healthy humans, emotionally-charged memory (i.e. enhanced memory for emotional events) shows large phenotypic variability [6] and has been linked to genetic variants of well-established neuromodulatory systems and molecules in candidate gene studies [6-13]. Similarly, there is substantial variability in the individual vulnerability to develop PTSD, particularly at lower levels of trauma exposure, which can be partially explained by genetic factors [14].

Next-generation sequencing coupled with efficient DNA capture has recently enabled the use of whole-exome sequencing (WES) to study the genetics of human phenotypes [15]. Indeed, WES studies have been particularly successful at identifying functional variants related to complex traits [15-17]. Such variants can be identified in a powerful way through extreme-phenotype sampling (EPS) followed by deep WES [17-20]. In EPS, a carefully selected population at one or both ends of the extremes of a phenotype, after adjustment for known covariates, is subjected to sequencing. In these populations, causal variants are expected to be enriched. Thus, even small

sample sizes may be sufficient to suggest candidate variants that can be subsequently genotyped in a larger group of phenotyped individuals, as also shown recently by empirical research [21].

Here we performed WES in healthy young subjects with extreme high or extreme low emotionally-charged memory performance, followed by targeted genotyping in a larger population showing normal distribution of the phenotype of interest (N = 2684). Genotype-dependent differences in emotional memory-related brain activation were studied in a homogenous sub-sample of 1258 subjects. In addition, we assessed the impact of the identified variants on gene expression in the post-mortem human brain and on symptoms and frequency of PTSD in genocide survivors.

Results

Exome sequencing in phenotypic extremes

Whole-exome sequencing (WES) was performed in 88 healthy young participants with extreme high or extreme low aversive memory performance carefully matched for sex (1-to-1 matching), genetic background, age, and smoking behavior (see Methods, Fig. 1, Fig. S1, Table S1). Aversive memory was quantified by means of a picture delayed free recall task. High- and low extremes were defined based on the distribution of aversive memory performance in N = 3418 healthy young subjects (see Methods).

WES was performed with the SureSelectXT Human All Exon V5+UTR target enrichment kit (Agilent), which allows for sequencing exonic and near-gene regulatory variants. To avoid discarding variants enriched to high frequency in the extremes [21], empirical minor allele frequency (MAF) in the extreme data set of N = 88 subjects was set to ≤ 0.125 (see Methods). Given that no prior information is available regarding putative differences in effect sizes of variants associated with the phenotype of interest, gene-based analyses were done by means of both burden and adaptive burden tests (see Methods). After adjustment for multiple testing, *TROVE2* (encoding TROVE Domain Family Member 2; Sjoegren Syndrome Type A Antigen; Ro60 KDa Autoantigen), *PKD2L2* (encoding Polycystin 2 Like 2, Transient Receptor Potential Cation Channel), and *CFAP57* (alias *WDR65;* encoding Cilia And Flagella Associated Protein 57) were significantly associated with group membership reflecting extreme aversive memory performance (Table 1). We

followed up on *TROVE2*, because this gene exceeded the adjusted significance threshold in both the burden and adaptive burden test (Table 1). In the burden test, its nominal significance survived Bonferroni correction for the entire number of genes (N = 21175) subjected to burden testing ($P_{nominal}$ = 2 x 10^{-6}, $P_{Bonferroni}$ = 0.042; Fig. S2). Moreover, *TROVE2* was the best hit ($P_{nominal}$ = 0.0002) on the Optimized Sequence Kernel Association Test (SKAT-O) [22] (Table S2). A detailed view of the sequencing data for *TROVE2* (Fig. 2) showed that the variant mainly responsible for the results of the gene burden tests was a 3'-UTR single nucleotide polymorphism (SNP) (rs72740218; C/T transition on chr1:193054088 according to GRCh37/hg19 coordinates). Ten of the 44 high extreme individuals were heterozygous minor *T* allele carriers, whereas this was the case for two of the 44 low extreme individuals. Pyrosequencing™-based genotyping confirmed this result (see Methods). According to the Exome Aggregation Consortium (ExAC) browser (version 0.3.1), rs72740218 MAF is 0.08 in European (Non-Finnish) populations. Free recall performance for positive material relative to neutral material (termed positive memory in analogy to aversive memory) was also significantly higher in high-extreme subjects. However, this was entirely due to this group's lower free recall performance for neutral pictures (Table S1). The genetic association findings were unrelated to the difference in positive memory between extreme groups: Firstly, TROVE2 was not significant (*P* = 0.6) when tested at the gene-level (SKAT-O with positive memory as quantitative phenotype). Secondly, TROVE2 variant rs6692342 was not significantly associated with positive memory (*P* = 0.2) or with free recall for positive pictures (*P* = 0.9).

Next, we tested whether the association of the *T* allele with increased aversive memory performance could be also detected in the entire population of healthy young subjects (N = 2684 successfully genotyped for rs72740218, including the N = 88 sequenced subjects, see Methods). We identified 19 minor allele homozygotes, 369 heterozygotes, and 2296 major allele homozygotes (empirical MAF = 0.075, Hardy-Weinberg $P > 0.1$). The *T* allele was significantly correlated ($P = 0.005$) with increased aversive memory performance, also after exclusion of the N = 88 sequenced extremes ($P = 0.035$, N = 2596). This sample of N = 2596 participants consisted of N = 217 subjects not selected for exome sequencing but nonetheless fulfilling the performance criteria for extreme high or extreme low aversive memory (Table S3), and of 2379 non-extreme individuals. Importantly, the significant association between rs72740218 and aversive memory performance in this population of N = 2596 participants was attributable to subjects exhibiting extreme aversive memory performance ($P = 0.0008$ for the interaction "genotype X extreme/non-extreme group membership"; r = 0.11 in N = 217 non-sequenced extremes; r = 0.016 in N = 2379 non-extremes).

Functional Brain Imaging (fMRI)

In the next step, we used fMRI to identify *TROVE2* rs72740218-dependent differences in brain activity related to memory encoding of aversive stimuli in N = 1258 subjects, a sub-sample of the population of N = 2596 healthy subjects (sequenced extremes excluded) who participated in the behavioral genetic study.

Importantly, all neuroimaging data were acquired in the same MRI scanner, thereby reducing hard- and software-related methodological variance.

We first investigated encoding-related brain activation independently of whether the information was later recalled or not (see Methods). We found significant [$P < 0.05$, two-sided test, family-wise error (FWE) corrected for whole brain] gene dose-dependent (i.e., with increasing number of the minor *T* allele) activity increases in the middle frontal gyrus, Brodmann area 9 (peak at [(-33, 36, 48), t = 5.39; $P(FWE_{corrected}) = 0.0015$]) (Fig. S3). Because these activation differences may be independent of memory processes, we then investigated brain activation related to *successful* memory encoding, i.e. activation specifically related to information that was later recalled (see Methods). We observed significant positive associations between *TROVE2* genotype (with increasing number of the minor *T* allele) and aversive memory-related activity in the left medial prefrontal cortex (peak at [(-5.5, 38.5, 36), superior frontal gyrus/paracingulate gyrus, Brodmann area 32, t = 5.80; $P(FWE) = 0.0003$; with FWE-corrected voxels extending to the dorsal anterior cingulate) (Fig. 3; Fig S4). Even after excluding the 6 minor allele homozygotes from the analysis, we found significant *TROVE2*-dependent activation differences between the major allele homozygotes and the heterozygotes with the peak at the same coordinate ([(-5.5, 38.5, 36), t = 5.25; $P(FWE) = 0.0125$]). There were no significant activity increases with increasing number of major alleles. Additionally, we tested if the reported association was specific for the negative valence. An analysis of *TROVE2*-dependent differences in brain activity related to successful memory encoding of positive stimuli as compared to neutral stimuli (see

Methods) did not reveal significant FWE-corrected results, nevertheless the corresponding uncorrected significance level was high ([(-5.5, 38.5, 36), t = 3.44; *P*(uncorrected) = 0.0006; *P*(FWE) = 0.97]). Accordingly, we did not observe significant [$P < 0.05$, two-sided test, FWE-corrected for whole brain] associations between the number of minor *TROVE2* alleles and contrast testing for brain activity differences between successful memory encoding of aversive vs. positive stimuli (see Methods), suggesting that, while the observed association was strongest for aversive stimuli, it was also observable for the positive valence.

In summary, the fMRI experiment revealed that the minor allele of *TROVE2 SNP* rs72740218, which was associated with increased memory for aversive information, was also related to increased brain activity in the medial prefrontal cortex during successful memory encoding of emotional pictures, with the strongest association being observed for aversive ones.

TROVE2 expression in human frontal cortex

Given the impact of *TROVE2* minor allele on brain activation related to successful memory encoding in the prefrontal cortex, we further investigated possible minor allele effects on *TROVE2* expression in this part of the human brain. For this analysis, we used the BRAINEAC data, a publicly available resource for the exploration of the regulatory significance of genetic variants in the human brain (http://www.braineac.org/) [23]. Brain samples specified as frontal cortex (FCTX) probes in the BRAINEAC database were taken from the prefrontal cortex (PFC),

198 mostly BA 9/46[24], a region well-known for its involvement in emotional processing
199 and -memory[25,26]. The 3'-UTR variant rs72740218 was significantly associated with
200 expression of the adjacent *TROVE2* terminal coding exon (exon-specific probeset
201 2372955; chr1:193053788-193053828, GRCh37/hg19 coordinates) in the PFC of
202 125 deceased subjects. The minor *T* allele predisposed to significantly higher
203 expression values (*P* = 0.005, Fig. 4A), possibly suggesting a local effect of this
204 variant on expression of the corresponding exon. No significance was observed at
205 the full transcript level (i.e., the Winsorised means over all exon-specific probesets)
206 (Table S4).
207
208 ***TROVE2* genetic variability in traumatized survivors of the Rwandan genocide.**
209 Extremely aversive, in particular life-threatening, incidents can lead to an excessive
210 and persisting emotional memory of the traumatic events, which can result in
211 intrusive and distressing re-experiencing (traumatic memory), a core PTSD
212 symptom. The heritability of re-experiencing traumatic events ranges from 23% to
213 51%, suggesting that naturally occurring genetic variations have an important
214 impact on this trait [27]. Given its association with aversive memory and aversive
215 memory-related brain activation in healthy subjects, we hypothesized that *TROVE2*
216 would be also associated with emotional memory for traumatic events reflected in
217 increased re-experiencing symptoms. We tested this hypothesis in 271 refugees
218 who have fled from the Rwandan civil war, have been living in the Nakivale refugee
219 camp in Uganda during the time of investigation, and from whom lifetime data on
220 the prevalence of PTSD was available (137 females, 134 males; mean age, 35 yrs;

range, 18–68 yrs, see Methods). All subjects had experienced highly aversive situations and were examined by trained experts with a structured interview based on the Posttraumatic Diagnostic Scale [28] with the help of trained interviewers chosen from the refugee community. Traumatic events were assessed using a checklist of 36 reported war- and non-war–related traumatic event types (e.g. injury by a weapon, rape, accidents) (Table S5). In Sub-Saharan African samples, variant rs72740218 is rare (MAF < 0.01 according to dbSNP). Therefore, we analyzed all *TROVE2*–spanning common SNPs present on the Human SNP Array 6.0 with an empirical MAF ≥ 0.05 in the Rwandan sample (N = 5 tagging SNPs, Table 2). None of these variants was significantly associated with age, sex, the number of experienced traumatic event types, or with the occurrence of any of the 36 distinct traumatic event types (Table 2, Table S5). *TROVE2* SNPs were significantly associated with traumatic memory (i.e., lifetime symptoms of re-experiencing the traumatic event) and with frequency of lifetime PTSD (Table 2). Variant rs6692342, located 555 and 1007 bases upstream of the respective *TROVE2* transcript variants (Fig. 5), showed the strongest association: minor allele *G* was associated with increased traumatic memory ($P = 0.007$) and with increased PTSD frequency ($P = 0.0004$). Linkage disequilibrium (LD) between variants rs6692342 and rs72740218 was not calculated in the PTSD sample, given the very low frequency of rs72740218 in the Rwandan population. In the Swiss sample, variants rs72740218 and rs6692342 were unlinked ($r^2 = 0.02$). Because the occurrence of some of the traumatic event types was unevenly distributed between rs6692342 genotype groups (albeit without reaching corrected statistical significance, Table S5), we

reran the analyses by controlling for such uneven distributions and obtained nearly identical results (Table S6). The minor allele *G* of variant rs6692342 was also modestly associated with increased expression of the adjacent *TROVE2* non-coding exon 1 of transcript variants NM_004600, NM_001173525, NM_001042369, and NM_001042370 (exon-specific probeset 2372928, chr1:193028950-193029112, GRCh37/hg19 coordinates) in the PFC of 123 deceased subjects of the BRAINEAC study ($P = 0.045$, Fig. 4B), possibly suggesting a local effect of this variant on expression of the corresponding exon. No significance was observed at the full transcript level (i.e., the Winsorised means over all exon-specific probesets) (Table S4). The frequency of the minor *G* allele of rs6692342 was nearly identical in the BRAINEAC and Rwandan samples (25.6% and 24.6%, respectively). Accordingly, rs6692342 genotype frequencies did not differ between these samples ($P = 0.5$, $\chi 2$ test). Importantly, genotype and allele frequencies in the BRAINEAC and Rwandan samples for rs6692342 were in close agreement with the respectively reported values for European and Sub-Saharan populations in the 1000 Genomes Project (Phase 3).

Discussion

The present study suggests that variants related to increased expression of *TROVE2* transcripts in the human frontal cortex are linked to emotional memory capacity and emotional memory-related brain activation in healthy subjects, and to traumatic memory and risk for PTSD in traumatized genocide survivors.

TROVE2 is widely expressed in human tissues, including the brain and its frontal cortex [23,29]. It undergoes complex transcriptional regulation, such as alternative splicing with several coding transcript variants and a range of 8-11 coding and non-coding exons [30,31] (Fig. 5). SNP rs72740218 was associated with emotional memory performance and brain activation related to successful memory encoding of emotionally-charged information in the medial prefrontal cortex, one of the key brain regions related to emotional processing[32], although it does not belong to one of the typical localizations found to be activated by emotional memory encoding in genotype-independent studies[33]. It is important to note, however, that genotype-independent analyses may not reveal brain regions for which different genotype groups show opposite activation patterns, e.g. when major allele homozygotes show a deactivation while the other genotype groups show an activation, as it was the case with SNP rs72740218 (Fig. S5). Importantly, is has been shown that PTSD patients as compared to controls show an increased response in the left dorsal anterior cingulate/medial prefrontal cortex at almost identical coordinate position (peak at -3, 39, 39) during encoding of later remembered negative verbal information[34]. Of note, there is evidence for a dissociative subtype of PTSD

283 patients, who typically show increased activation in the anterior cingulate/medial
284 PFC)[35].
285 SNP rs72740218 is located within the 3'-UTR of transcripts NM_001173524 and
286 NM_004600 (Fig. 5), and is significantly associated with expression levels of the
287 terminal coding exon of these variants in the PFC (Fig. 4). SNP rs6692342, which
288 was associated with traumatic memory and PTSD frequency, is located 555 bases
289 upstream of transcript variant NM_001173524 and 1007 bases upstream of
290 transcript variants NM_004600, NM_001173525, NM_001042369, and
291 NM_001042370, and is modestly, albeit significantly associated with expression
292 levels of the adjacent non-coding exon 1 of the latter four variants in the PFC (Fig.
293 4). Taken together, the minor alleles of these *TROVE2* SNPs were associated with
294 increased expression of adjacent exons and with gain of emotional (in the case of
295 rs72740218) and traumatic (in the case of rs6692342) memory-related phenotypes.
296 Given that free recall was assessed shortly after encoding in this study, further
297 research will be needed to study the gene's role on emotional memory capacity
298 related to longer-term (e.g. hours, days) consolidation processes.
299 *TROVE2* encodes Ro60, an RNA-binding protein that binds to misfolded non-coding
300 RNAs, pre-5S rRNA, and Y RNAs [31]. Autoantibodies to Ro60 are prevalent in
301 autoimmune disorders including Sjögren's syndrome and systemic lupus
302 erythematosus (SLE) [36-38], and recent research argues in favor of a direct link
303 between Ro60 autoantibody production, type I interferon, and autoimmunity [39].
304 The findings of the present study argue in favor of a genetic link between *TROVE2*
305 and emotional memory-related traits, possibly via regulation of specific transcripts.

306 Although speculative, one might hypothesize that *TROVE2* plays a role in a possible
307 link between the regulation of immune-related processes and the regulation of
308 emotional memory-related traits, given the gene's crucial involvement in
309 autoimmunity. Importantly, recent genetic and epidemiological data point to a link
310 between autoimmunity and PTSD: a retrospective cohort study of 666,269 Iraq and
311 Afghanistan veterans revealed significant associations between PTSD and risk for
312 autoimmune disorders, with shared etiology being one of the possible explanations
313 for this observation [40]. Very recently, a large genome-wide association study
314 (GWAS) of PTSD revealed a significantly increased enrichment ratio for immune-
315 related expression quantitative trait loci in PTSD [41]. In addition, abnormal cytokine
316 regulation and a proinflammatory milieu are present in PTSD[42-45]. Thus, a link
317 between the regulation of immune functions and emotional memory-related
318 neuropsychiatric phenotypes is likely to exist. Despite the known, direct connection
319 between the human brain and peripheral tissues relevant to the function of the
320 immune system [46], it is not possible to draw yet any causal inferences about the
321 mechanistic nature of this link and about a putative involvement of *TROVE2*.
322 Interestingly, recent animal research identified meningeal immunity as a direct
323 player in the regulation of such complex brain functions as learning, memory, and
324 social behavior [47,48].
325 A number of -mostly small- PTSD GWAS in civilian and military or veteran samples
326 have been published[41,49-55]. *TROVE2* has not been reported as one of the top hits in
327 these GWAS. Of note, the published GWAS results do not converge so far. It is
328 widely acknowledged that substantial within- and between-sample differences in

329 traumatic event type, duration, and rate, time of trauma onset, ancestry,
330 sociodemographic factors, and social support render comparability of GWAS
331 results in the PTSD field inherently difficult[56]. The possibility exists that some of the
332 reported findings might prove specific to a certain population. Thus, the replication
333 issue of genetic studies of PTSD will remain challenging and might be resolved by
334 future large collaborative efforts, which should include different subgroups of large
335 homogenous samples. Interestingly, a recent study reporting on combined genetic
336 and transcriptomic findings in human and *C. elegans* identified *TROVE2* as one of
337 the top scoring genes involved in mood regulation and stress response[57].
338 In the present study we used exome sequencing in healthy phenotypic extremes to
339 detect genes linked to emotionally-charged memory capacity. Importantly, the
340 extreme phenotype design proved to be crucial for the identification of *TROVE2*,
341 because the effect size of the minor allele *T* of rs72740218 was considerably higher
342 in the extremes, also the non-sequenced ones, compared to the largest, middle
343 part of the phenotypic distribution. It is important to stress that the success of the
344 genetic search presented herein is not necessarily generalizable to every
345 genetically complex cognitive/emotional trait. A synergy of such factors as
346 meticulous matching of phenotypic extremes with particular focus on genetic
347 background [15], a relatively high MAF for the implicated variant, and the specific
348 genetic architecture of the phenotype of interest gave rise to the identification of
349 *TROVE2*. Nevertheless, our experience with this approach and the statistical
350 features of our findings are in close analogy to the respective observations of a

recent study which identified a genetic modifier of a Mendelian trait (cystic fibrosis) by means of exome sequencing in phenotypic extremes [21].

In conclusion, *TROVE2*, a gene implicated in autoimmunity, is linked to emotionally-charged memory in health and psychiatric disease, particularly PTSD. Specifically, the present findings suggest that the price for the *TROVE2* variant-related enhancement of emotional memory is enhanced intrusive and distressing memory for traumatic events. Given that many mental disorders represent the extremes of a normal distribution of traits on multiple cognitive and emotional dimensions [58], we believe that appropriate genetic methodologies in healthy phenotypic extremes may help uncover disease dimensions with different symptom patterns, a subtyping that may be necessary to improve understanding and treatment of psychopathology.

Methods

Definition of phenotypic extremes

Aversive memory was assessed in N = 3418 subjects who participated in ongoing behavioral and imaging genetics studies of healthy young adults in the city of Basel, Switzerland (Data lock Apr. 2015). The ethics committee of the Cantons of Basel-Stadt and Basel-Landschaft approved the experiments. All participants received general information about the study and gave their written informed consent for participation. Participants were free of any neurological or psychiatric illness, and did not take any medication at the time of the experiment (except hormonal contraceptives).

Aversive memory was quantified by means of a picture delayed free recall task. Stimuli consisted of 72 pictures that were selected from the International Affective Picture System (IAPS) [59] as well as from in-house standardized picture sets that allowed us to equate the pictures for visual complexity and content (e.g. human presence). On the basis of normative valence scores (from 1 to 9), pictures were assigned to emotionally negative (2.3 ± 0.6), emotionally neutral (5.0 ± 0.3), and emotionally positive (7.6 ± 0.4) conditions, resulting in 24 pictures for each emotional valence. Four additional pictures showing neutral objects were used to control for primacy and recency effects in memory. Two of these pictures were presented in the beginning and two at the end of the picture task. They were not included in the analysis. The pictures were presented for 2.5 s in a quasi-randomized order. To ensure that the ratio between valence categories was kept

386 constant across consecutive parts of the entire picture sequence, each twelfth part
387 of the sequence contained exactly two positive, two negative, and two neutral
388 pictures. Thus, maximally four pictures of the same category occurred
389 consecutively. Ten minutes after picture presentation, memory performance was
390 tested using a free-recall task, which required participants to write down a short
391 description (a few words) of the previously seen pictures. Remembered primacy
392 and recency pictures as well as training pictures were excluded from the analysis.
393 No time limit was set for this task. A picture was scored as correctly recalled, if the
394 rater could identify the presented picture on the basis of the subject's description.
395 Two trained investigators independently rated the descriptions for recall success
396 (inter-rater reliability >99%). A third independent rater decided on pictures, which
397 were rated differently [7]. For the purpose of selecting phenotypic extremes,
398 aversive memory performance was calculated by subtracting the number of the
399 freely recalled neutral pictures from the number of freely recalled negative
400 pictures. In a sub-sample of 1900 subjects with data on a second assessment of
401 free recall performance 24h after the first presentation of the identical picture set,
402 both phenotypes showed high levels of inter-trial correlation (Pearson's r = 0.73
403 and r = 0.78 for free recall of negative and neutral pictures, respectively). Based on
404 the observed phenotypic distribution, subjects with aversive memory performance
405 ≥ 10 and ≤ 13 were classified as high-extreme subjects (HES), and subjects with
406 aversive memory performance ≥ -5 and ≤ -1 were classified as low-extreme
407 subjects (LES). We adopted an almost-extreme sampling approach, because the
408 very extremes of cognitive phenotypes are vulnerable to potential measurement

errors and phenotype heterogeneity [18]. For example, performance at the very extreme low end of the distribution might be related to erroneous understanding of task instructions or to gross errors in task execution. Moreover, the additive polygenic mode of inheritance of common phenotypes breaks down at the very extremes of the distribution tails[60,61]. Thus, subjects at the very extreme ends, as identified upon visual inspection of the frequency histogram (i.e., aversive memory performance < -5, N = 6; aversive memory performance > 13, N = 8), were not considered for further analysis (Fig. 1).

Next, we selected all subjects who had been genotyped on the Genome-Wide Human SNP Array 6.0 (Affymetrix®) and performed standard quality control (QC) with PLINK (http://pngu.mgh.harvard.edu/~purcell/plink) including sex check and identity by descent analysis as described in [62], resulting in N = 2991 subjects with QC'd SNP array data.

The next steps were performed to calculate each subject's genetic background, to select a homogeneous group of participants of European ancestry, and to compute an individual parameter in order to match the to-be-sequenced extremes for genetic similarity. Thus, we analyzed the SNP array data of seven Swiss and German samples [62-64] (total *N* = 5172) including our target sample. Genetic data of these subjects was projected onto the first two principal components (PCs) of genetic variation in the HapMap3 reference sample (consisting of African, Asian, and European samples) using SMARTPCA [65]. Participants scoring on PC1 < 0.012 and on PC2 < 0.065 were then filtered out to obtain a cluster of broad European ancestry (Fig. S1A,B). Genetic data of the subjects composing this cluster was also

checked for the presence of duplicates and cryptic relatedness (IBD: $\hat{p} < 0.2$). Before performing the final principal component analysis (PCA) within this European sample, genetic QC (*MAF* > 0.02, *CR* > 0.95, $p_{HWE} > 0.001$) was applied within each of the seven sub-samples separately. We also excluded SNPs within regions of long-range linkage disequilibrium (LD) as suggested by [66]. The remaining autosomal SNPs of the combined sample were then pruned using PLINK (indep-pairwise command; window-size 200 SNPs, 5 SNP steps, $r^2 < 0.2$). We next used SMARTPCA [65] to estimate the principal components of genetic variation within this broad European cluster (Fig. S1A,B). The resulting first two PCs were used as parameters for genetic similarity.

After these steps, N = 2739 subjects of European ancestry remained for further selection of pairs of subjects from the high- and low extreme groups that: 1) have a similar genetic background; 2) have the same sex; 3) were investigated at a similar time-point; 4) are of similar age; 5) have similar smoking behavior. The latter matching criterion was included given the borderline significant correlation between smoking status and being a member of the high- or low extreme performance group (P=0.08 before matching). Matching was done separately for females and males with the library Matching (Version 4.8-3.4) in R [67]. Membership in the low- or high extreme group was used as treatment vector. Matching was done without replacement, the sequence of the subjects entering the matching procedure was chosen randomly. Time-point of investigation, age, smoking behavior and the two results of the first two PCs from the genetic similarity analysis were used as variables to match on. For each HES, the best-matching LES

455 was identified, separately for females and males. Finally, these high extreme-low
456 extreme pairs were randomly assigned on the plate for subsequent exome
457 sequencing. In line with the circumstance that emotionally arousing information is
458 often remembered at the expense of neutral background information[68], HES had
459 significantly increased mean free recall performance for aversive pictures (P = 3 x
460 10^{-17}) and significantly, albeit orders of magnitude weaker, decreased mean free
461 recall performance for neutral pictures (P = 1 x 10^{-12}) than LES (Table S1). No
462 difference in mean free recall performance for positive pictures (P = 0.6) was
463 observed between HES and LES. Overall memory capacity was very similar between
464 extreme groups (P = 0.5). There was no difference in mean free recall performance
465 for positive pictures between HES and LES (P = 0.6). No significant group difference
466 in arousal and valence ratings for any of the 3 picture categories was observed (all
467 P's > 0.05).
468
469 **Exome sequencing: Blood sampling, DNA isolation and related QCs**
470 Blood samples were collected between midday and evening (mean time of day:
471 2:30 p.m., range 1:00 p.m. – 8.00 p.m.) using BD Vacutainer® Push Button blood
472 collection sets and 10.0 mL BD Vacutainer® Plus plastic whole blood tubes, BD
473 Hemogard™ closure with spray-coated K_2EDTA (Becton, Dickinson and Company ,
474 New Jersey, USA). Standard hematological analysis, including blood cell counting,
475 was performed with Sysmex pocH-100*i*™ Automated Hematology Analyzer (Sysmex
476 Co, Kobe, JP.) DNA was isolated from the remaining fraction, upon plasma removal.
477 The isolation was performed with QIAmp Blood Maxi Kit (Qiagen AG, Hilden,

Germany), using the recommended spin protocol. In order to obtain high purity DNA, isolated DNA samples were additionally re-purified. For this purpose, 2 g of DNA isolated with QIAmp/Oragene procedure, was incubated overnight at 50°C with proteinase K (Lysis buffer: 30 mM Tris·Cl; 10 mM EDTA; 1% SDS, pH 8.0; 150ng/ l Proteinase K), agitated by gentle orbital shaking. Next, DNA was purified using Genomic DNA Clean & Concentrate Kit (Zymo Research, Irvine, CA USA). The quality and concentration of DNA were assessed using gel electrophoresis, NanoDrop ND-1000 (Thermo Scientific, Waltham, MA, USA) and fluorometry measurements (Qubit dsDNA BR Assay Kit; Invitrogen, Carlsbad, CA USA), respectively. DNA samples of high integrity and purity were further normalized to 24ng/ l and randomly assigned to a 96-well plate for library preparation.

Exome sequencing: Library preparation

Quality checks of the genomic DNA samples and intermediate products of the library preparation (efficiency of DNA fragmentation, pre and post capture libraries) were done with the Fragment Analyzer, using the DNF-467 Genomic DNA 50 Kb Analysis Kit and DNF-473 Standard Sensitivity NGS Fragment Analysis Kit, respectively (Advanced Analytical Technologies, IA, USA). Library preparation for whole-exome sequencing was performed with the Agilent SureSelectXT Human All Exon V5+UTR kit using the SureSelectXT automated target enrichment for Illumina paired-end multiplexed sequencing protocol on the Agilent NGS workstation, option B (Agilent Technologies Inc, CA, USA). In short, 200ng of genomic DNA was fragmented with the Covaris E220 Focused-ultrasonicator (Covaris Inc, MA, USA),

501 with the following settings: Duty Factor - 10%; Peak Incident Power – 175; Cycles
502 per Burst – 200; Treatment Time -360s; Bath Temperature 4° to 8° C. The target
503 DNA fragment size was 150 to 200 bp. After quality assessment the libraries were
504 further prepared by using the SureSelect XT Library Prep Kit ILM (Agilent, USA;
505 SureSelectXT Target Enrichment System for Illumina Paired-End Multiplexed
506 Sequencing Library Protocol version B3). AMPure XP beads purification was always
507 implemented between the library preparation steps. First, the 3' ends of the DNA
508 fragments were adenylated, followed by paired-end adaptor ligation and adaptor-
509 ligated library amplification. After library quality assessment, samples were
510 hybridized to the target-specific capture library and the hybridized DNA was
511 captured with streptavidin-coated beads. The libraries with 8-bp indexing primers
512 were then amplified, assayed for quality and quantity and finally pooled for
513 multiplexed sequencing.
514
515 **Whole-exome sequencing (WES)**
516 Libraries were clustered on the Illumina cBot cluster station (HiSeq PE Cluster Kit
517 v4). WES was done on an Illumina HiSeq 2500 machine (paired-end reads, 101bp
518 per read). The libraries were mixed in 4 pools (3x24 + 1x22). Each pool was
519 sequenced in 6 lanes. A fifth pool was mixed with 27 of the samples and this Pool 5
520 was sequenced in an extra lane. For each sample, over 12GB of sequence were
521 generated.
522 The SureSelectXT Human All Exon V5+UTR kit (Agilent) used in this study targets
523 359555 exons in 21522 genes (i.e. 75Mb of sequence) included in following

databases: CCDS, RefSeq, GENCODE, miRBase, TCGA and UCSC. Each sample's sequence was mapped to the hg19 human reference genome, downloaded from http://genome.ucsc.edu, using BWA 0.7.12 (Burrow-Wheeler Alignment) [69]. Duplicates were flagged with Picard 1.135 (http://picard.sourceforge.net). Analysis of coverage was done with Picard CalculateHSmetrics and Bedtools 2.18.1[70]. 98% of the target bases had a coverage equal or greater than 20X and ~ 50% of target bases had 100X coverage (Bedtools; Fig. S6). Base quality score recalibration and local realignment around indels was done with GATK 3.4-0 [71] following the standard GATK protocol [72]. SNVs were called with the Haplotype Caller. No padding was used for variant calling outside non-target regions to prevent false positive SNV calls. Following the recommendation of DePristo et al [73], Variant Quality Score Recalibration (VQSR) was used. We chose 99% sensitivity for a variant to be "true" based on an adaptive error model and filtered out false-positive variants upon this threshold.

Exome sequencing: Callset quality control

The final callset was evaluated using variant-level concordance (i.e. percentage of variants in the study sample matching a defined gold standard) and genotype concordance (i.e. percentage of variants matching the genotypes derived from the same samples using a different genotyping technique). After defining dbSNP 138.b37 as the gold standard, we ran GATK's VariantEval toolkit. The variant-level concordance rate between our callset and dbSNP was high (98.33%). Two genotype concordance measures can be derived from comparing sequencing data with array

data: Non-reference sensitivity (NRS, i.e. rate at which non-reference alleles in the array data are also identified in the sequenced genotypes) and the non-reference discrepancy rate (NRD; i.e. the rate at which sequenced genotypes differ from array genotypes). We used the GATK toolkit GenotypeConcordance for these calculations. 18'709 bi-allelic overlapping variants were identified for both WES data and array genotype data of the Affymetrix 6.0 human SNP array. NRS was 97.5%, suggesting a high sensitivity for common variants, and NRD was 2.4%. The ratio between transitions to transversions (Ti/Tv ratio) was 2.61, well matching the expected value between 2.5 and 2.8 for sequences covering both exonic and non-exonic 3' and 5' UTRs [74], like the SureSelectXT Human All Exon V5+UTR kit (Agilent), that targets 75Mb of the human genome. We furthermore checked the rate of novel missense SNPs (i.e. not included in dbSNP 138.b37) in our callset. The mean over all samples was low (n=57.8), suggesting a low number of false-positive calls. Another quality indicator is the het/hom ratio (i.e. the ratio between heterozygous and homozygous non-reference variants). In our callset, the het/hom ratio, which is expected to be approximately 1.5 for European populations [75,76], was 1.57 for all SNPs and 1.54 for known SNPs (i.e. dbSNP SNPs). Variant Call Format (VCF) data were annotated with the reference genome GRCh37.75 using SnpEff software (4.1l (build 2015-10-03) [77].

Pyrosequencing

Targeted genotyping of *TROVE2* SNP rs72740218 was done with Pyrosequencing on a PyroMark™ ID System. Following primers were used: 5'- TAC TAA ACT AGC TCT

570 TGG GGA AAT -3' (forward primer, 5'-biotinylated), 5'- CAA AGC AAA ACT ATT TTA
571 CAG TGT -3' (reverse primer), 5'- CAA AAA GTT CTC TAT TAG AT -3' (sequencing
572 primer). N = 2684 subjects were successfully genotyped for rs72740218. One-sided
573 genetic association testing (additive model) was used for hypothesis confirmation
574 purposes. Researcher team members involved in genotyping were blinded to group
575 allocation.
576
577 **Burden Testing**
578 Genotype-phenotype associations were calculated with PLINK7SEQ v0.10
579 (https://atgu.mgh.harvard.edu/plinkseq/). We calculated gene-based tests falling
580 into two categories: burden tests [78] and adaptive burden tests (variable threshold
581 test VT) [79]. Burden tests perform optimally assuming that a large proportion of
582 variants are causal and the effects are in the same direction. Adaptive burden tests,
583 which use data-adaptive weights or thresholds, are thought to be more robust than
584 burden tests using fixed weights or thresholds [80]. Following power analyses done in
585 studies of phenotypic extremes with similar sample size as in the present one, we
586 set the empirical minor allele frequency (MAF) to ≤ 0.125 to avoid eliminating
587 variants enriched to high frequency in the extremes [21]. To correct for multiple
588 testing we used the i-stat statistic (i.e. a gene's smallest possible empirical p-value),
589 which is implemented in PLINKSeq. According to previous recommendations, i-stat
590 threshold was set to <0.001 [15]. Burden test-derived significances were then
591 Bonferroni-corrected for the number of genes with i-stat below this threshold.
592

fMRI experiment

Subjects were right-handed, free of any lifetime neurological or psychiatric illness, and did not take any medication (except hormonal contraceptives) at the time of the experiment, which was approved by the ethics committee of the Cantons of Basel-Stadt and Basel-Landschaft. Written informed consent was obtained from all subjects prior to participation. After receiving general information about the study and giving their informed consent, participants were instructed and then trained on the picture task they later performed in the scanner. After training, they were positioned in the scanner. The participants received earplugs and headphones to reduce scanner noise. Their head was fixated in the coil using small cushions, and they were told not to move their heads. Functional MR-images were acquired during the performance of the picture task in two separate sessions (total scanning time approximately 30 min). After finishing the tasks, participants left the scanner and were taken to a separate room for free recall of the pictures. Finally, participants filled out questionnaires, gave saliva for genotype analysis and were debriefed. The total length of the experimental procedure was approximately 3 hours. We excluded 54 subjects from the fMRI experiment. Reasons for exclusion were defined as follows: corrupted or missing data (N=40), subjects recalling less than one picture in one of the valence categories (N=10), failed co-registration (N = 4).

Measurements were performed on a Siemens Magnetom Verio 3 T wholebody MR unit equipped with a twelve-channel head coil. Functional time series were

616 acquired with a single-shot echo-planar sequence using parallel imaging (GRAPPA).
617 We used the following acquisition parameters: TE (echo time) = 35 ms, FOV (field
618 of view) = 22 cm, acquisition matrix = 80 × 80, interpolated to 128 × 128, voxel size:
619 2.75 × 2.75 × 4 mm3 , GRAPPA acceleration factor R = 2.0. Using a midsagittal scout
620 image, 32 contiguous axial slices were placed along the anterior–posterior
621 commissure (AC–PC) plane covering the entire brain with a TR = 3000 ms (= 82°).
622 The first two acquisitions were discarded due to T1 saturation effects. A high-
623 resolution T1-weighted anatomical image was acquired using a magnetization
624 prepared gradient echo sequence (MPRAGE, TR=2000 ms; TE=3.37 ms; TI=1000 ms;
625 flip angle=8; 176 slices; FOV= 256 mm; voxel size=1 x 1 x 1 mm3).
626 Preprocessing and data analysis was performed using SPM8 (Statistical Parametric
627 Mapping, Wellcome Department of Cognitive Neurology, London, UK;
628 http://www.fil.ion.ucl.ac.uk/spm/) implemented in Matlab (The Mathworks Inc.,
629 Natick, MA, USA). Volumes were slice-time corrected to the first slice and realigned
630 to the first acquired volume. Both functional and structural images were spatially
631 normalized by applying DARTEL, which leads to an improved registration between
632 subjects. Normalization incorporated the following steps: 1. Structural images of
633 each subject were segmented using the “New Segment” procedure in SPM8. 2. The
634 resulting gray and white matter images were used to derive a study-specific group
635 template. The template was computed from a subpopulation of 1000 subjects from
636 this study. 3. An affine transformation was applied to map the group template to
637 MNI space. 4. Subject-to-template and template-to-MNI transformations were
638 combined to map the functional images to MNI space. The functional images were

639 smoothed with an isotropic 8 mm full width at half maximum (FWHM) Gaussian
640 filter. Serial correlations were removed using a first-order autoregressive model. A
641 high-pass filter (128 s) was applied to remove low-frequency noise.
642 Normalized functional images were masked using information from their
643 respective T1 anatomical file as follows: A partial volume effect file obtained from
644 the SPM-VBM8 toolbox (http://dbm.neuro.uni-jena.de/vbm8/) was used as
645 starting point to define the brain mask. This volume represents the three-tissue
646 classification results of the segmentation process (GM, WM, CSF), with two
647 additional mixed classes (GM-WM, GM-CSF). It was binarized, dilated and eroded
648 with a 3x3x3 voxels kernel using FSL's *fslmaths* to fill in potential small holes in the
649 mask. The previously computed DARTEL flowfield was used to normalize the brain
650 mask to MNI space, at the spatial resolution of the functional images. The mask
651 was finally thresholded at 10% and applied to the normalized functional images.
652 Consequently, the implicit intensity-based masking threshold usually employed to
653 compute a brain mask from the functional data during the first level specification
654 (by default fixed at mask.thresh=0.8) was not needed any longer and set to a lower
655 value of 0.05.
656 For each subject, analyses were conducted in the framework of the general linear
657 model (GLM). Regressors modeling the onset and duration of stimulus events were
658 convolved with a canonical hemodynamic response function. More precisely, the
659 model comprised regressors for button presses modeled as stick/delta functions,
660 picture presentations modeled with an epoch/boxcar function (duration: 2.5s), and
661 rating scales modeled with an epoch/boxcar function of variable duration

(depending on when the subsequent button press occured). Six movement parameters were also entered as nuisance covariates. Pictures accounting for possible primacy and recency effects were modeled separately.

Brain activity contrasts were calculated individually using a fixed effects model (first level analysis). The following contrasts were specified: (i) brain activity related to memory encoding of aversive stimuli as compared to neutral stimuli, independent of whether the information was later recalled or not *(aversive pictures - neutral pictures).* (ii) brain activity related to successful memory encoding of aversive stimuli as compared to neutral stimuli *(aversive pictures recalled - aversive pictures not recalled) – (neutral pictures recalled – neutral pictures not recalled)*; (iii) differences in brain activity between successful memory encoding of aversive vs. positive stimuli *(aversive pictures recalled – aversive pictures not recalled) – (positive pictures recalled – positive pictures not recalled);* (iv) brain activity related to successful memory encoding of positive stimuli as compared to neutral stimuli *(positive pictures recalled - positive pictures not recalled) – (neutral pictures recalled – neutral pictures not recalled)*. The resulting contrast parameters were then used for genotype-dependent analyses in a random effects model (second level analysis). Specifically, we used a regression model to analyze differences in brain activity, whereas the number of alleles served as covariate in our analysis. We controlled for the effects of sex and age by including them as covariates. Significance peaks were assigned to anatomical labels based on the Harvard-Oxford Cortical Structural Atlas[81]. Brodmann areas are given based on[82].

Rwanda sample

Study participants were survivors of the Rwandan genocide who were living as refugees in the Nakivale refugee settlement As the Nakivale refugee settlement has grown over the last decade and is spread over a large area, participants were sampled proportionally to the population size from each zone. To exclude genetic relatives in the samples, only one person per household was interviewed. Interviewers had been trained to detect current alcohol abuse and acute psychotic symptoms; candidates exhibiting these signs were excluded. All subjects had experienced highly aversive traumatic situations (including life-threatening situations) and were examined in 2006/2007 by psychologists of the University of Konstanz with the help of trained interpreters, or by intensely trained local interviewers using a structured interview based on the Posttraumatic Diagnostic Scale (PDS) [28] with the help of trained interpreters. This procedure has been validated for implementation in East African crisis regions [83]. Traumatic events were assessed with a checklist of 36 war- and non-war-related traumatic event types, e.g. injury by weapon, rape, accident, which has been also employed in previous studies [7]. Traumatic load was estimated by assessing the number of different *traumatic event types* experienced or witnessed. This measure has been shown to be more reliable than assessing the frequency of traumatic events [84]. The procedures and study protocols were approved by the Ethics Committees of the University of Konstanz, Germany, and the Mbarara University of Science and Technology (MUST), Mbarara, Uganda.

Instruments were translated into Kinyarwanda using several steps of translations, blind back-translations, and subsequent corrections by independent groups of translators. Following the translations, the psychometric properties of the translated scales were investigated in a validation study including a retest spanning a two-week period and a cross-validation with expert rating [85]. To avoid known ceiling effects (i.e. the phenomenon that almost everybody will develop PTSD at extreme levels of trauma load) [86,87], subjects were selected to have experienced no more than 16 different traumatic event types. Subjects lacking sufficient data for the estimation of the prevalence of lifetime PTSD were excluded from this study. The significance level of genetic associations with traumatic memory and PTSD risk was calculated by performing forward and backward linear and logistic regressions, respectively, under inclusion of age, sex, trauma load, and –wherever indicated- occurrence of specific traumatic event types. The significance level of genetic associations with trauma load and the occurrence of specific traumatic events was calculated by performing forward and backward linear and logistic regressions, respectively, under inclusion of age and sex. The significance level of genetic associations with age and sex was calculated by performing linear regressions and χ^2 tests, respectively. Saliva samples were obtained from each person using Oragene™ DNA Self-Collection Kit (DNA Genotek, Ottawa, Ontario Canada). DNA was extracted from saliva using standard protocols.

Data availability. The data that support the findings of this study are available from the corresponding author upon request.

References

1. McGaugh, J.L. The Making of Lasting Memory. in *Memory and Emotion* (Weidenfeld and Nicolson, London, 2003).
2. Pitman, R.K. Post-traumatic stress disorder, hormones, and memory. *Biol Psychiatry* **26**, 221-223 (1989).
3. Phelps, E.A. & LeDoux, J.E. Contributions of the amygdala to emotion processing: from animal models to human behavior. *Neuron* **48**, 175-187 (2005).
4. Brewin, C.R., Dalgleish, T. & Joseph, S. A dual representation theory of posttraumatic stress disorder. *Psychol Rev* **103**, 670-686 (1996).
5. Brewin, C.R., Gregory, J.D., Lipton, M. & Burgess, N. Intrusive images in psychological disorders: characteristics, neural mechanisms, and treatment implications. *Psychol Rev* **117**, 210-232 (2010).
6. de Quervain, D.J*., et al.* A deletion variant of the alpha2b-adrenoceptor is related to emotional memory in Europeans and Africans. *Nat Neurosci* **10**, 1137-1139 (2007).
7. de Quervain, D.J*., et al.* PKCalpha is genetically linked to memory capacity in healthy subjects and to risk for posttraumatic stress disorder in genocide survivors. *Proc Natl Acad Sci U S A* **109**, 8746-8751 (2012).
8. Todd, R.M*., et al.* Deletion variant in the ADRA2B gene increases coupling between emotional responses at encoding and later retrieval of emotional memories. *Neurobiol Learn Mem* **112**, 222-229 (2014).
9. Todd, R.M., Palombo, D.J., Levine, B. & Anderson, A.K. Genetic differences in emotionally enhanced memory. *Neuropsychologia* **49**, 734-744 (2011).
10. Papassotiropoulos, A*., et al.* Human genome-guided identification of memory-modulating drugs. *Proc Natl Acad Sci U S A* **110**, E4369-4374 (2013).
11. Ackermann, S., Heck, A., Rasch, B., Papassotiropoulos, A. & de Quervain, D.J. The BclI polymorphism of the glucocorticoid receptor gene is associated with emotional memory performance in healthy individuals. *Psychoneuroendocrinology* **38**, 1203-1207 (2013).
12. Gibbs, A.A., Bautista, C.E., Mowlem, F.D., Naudts, K.H. & Duka, T. Alpha 2B adrenoceptor genotype moderates effect of reboxetine on negative emotional memory bias in healthy volunteers. *J Neurosci* **33**, 17023-17028 (2013).
13. Cheung, J. & Bryant, R.A. FKBP5 risk alleles and the development of intrusive memories. *Neurobiol Learn Mem* **125**, 258-264 (2015).
14. Wilker, S., Elbert, T. & Kolassa, I.T. The downside of strong emotional memories: how human memory-related genes influence the risk for posttraumatic stress disorder--a selective review. *Neurobiol Learn Mem* **112**, 75-86 (2014).
15. Kiezun, A*., et al.* Exome sequencing and the genetic basis of complex traits. *Nat Genet* **44**, 623-630 (2012).

16. Wang, Z., Liu, X., Yang, B.Z. & Gelernter, J. The role and challenges of exome sequencing in studies of human diseases. *Front Genet* **4**, 160 (2013).
17. Peloso, G.M*., et al.* Phenotypic extremes in rare variant study designs. *Eur J Hum Genet* **24**, 924-930 (2016).
18. Li, D., Lewinger, J.P., Gauderman, W.J., Murcray, C.E. & Conti, D. Using extreme phenotype sampling to identify the rare causal variants of quantitative traits in association studies. *Genet Epidemiol* **35**, 790-799 (2011).
19. Auer, P.L. & Lettre, G. Rare variant association studies: considerations, challenges and opportunities. *Genome Med* **7**, 16 (2015).
20. Guey, L.T*., et al.* Power in the phenotypic extremes: a simulation study of power in discovery and replication of rare variants. *Genet Epidemiol* **35**, 236-246 (2011).
21. Emond, M.J*., et al.* Exome sequencing of extreme phenotypes identifies DCTN4 as a modifier of chronic Pseudomonas aeruginosa infection in cystic fibrosis. *Nat Genet* **44**, 886-889 (2012).
22. Lee, S*., et al.* Optimal unified approach for rare-variant association testing with application to small-sample case-control whole-exome sequencing studies. *Am J Hum Genet* **91**, 224-237 (2012).
23. Ramasamy, A*., et al.* Genetic variability in the regulation of gene expression in ten regions of the human brain. *Nat Neurosci* **17**, 1418-1428 (2014).
24. Trabzuni, D*., et al.* Quality control parameters on a large dataset of regionally dissected human control brains for whole genome expression studies. *J Neurochem* **119**, 275-282 (2011).
25. LaBar, K.S. & Cabeza, R. Cognitive neuroscience of emotional memory. *Nat Rev Neurosci* **7**, 54-64 (2006).
26. Buchanan, T.W. Retrieval of emotional memories. *Psychol Bull* **133**, 761-779 (2007).
27. Stein, M.B., Jang, K.L., Taylor, S., Vernon, P.A. & Livesley, W.J. Genetic and environmental influences on trauma exposure and posttraumatic stress disorder symptoms: a twin study. *Am J Psychiatry* **159**, 1675-1681 (2002).
28. Foa, E.B., Cashman, L., Jaycox, L. & Perry, K. The validation of a self-report measure of posttraumatic stress disorder: The Posttraumatic Diagnostic Scale. *Psychol Assess* **9**, 445-451 (1997).
29. Hawrylycz, M.J*., et al.* An anatomically comprehensive atlas of the adult human brain transcriptome. *Nature* **489**, 391-399 (2012).
30. Speir, M.L*., et al.* The UCSC Genome Browser database: 2016 update. *Nucleic Acids Res* **44**, D717-725 (2016).
31. UniProt, C. UniProt: a hub for protein information. *Nucleic Acids Res* **43**, D204-212 (2015).
32. Etkin, A., Egner, T. & Kalisch, R. Emotional processing in anterior cingulate and medial prefrontal cortex. *Trends Cogn Sci* **15**, 85-93 (2011).
33. Murty, V.P., Ritchey, M., Adcock, R.A. & LaBar, K.S. fMRI studies of successful emotional memory encoding: A quantitative meta-analysis. *Neuropsychologia* **48**, 3459-3469 (2010).

34. Thomaes, K.*, et al.* Increased anterior cingulate cortex and hippocampus activation in Complex PTSD during encoding of negative words. *Soc Cogn Affect Neurosci* **8**, 190-200 (2013).
35. Lanius, R.A.*, et al.* Emotion modulation in PTSD: Clinical and neurobiological evidence for a dissociative subtype. *Am J Psychiatry* **167**, 640-647 (2010).
36. Schulte-Pelkum, J., Fritzler, M. & Mahler, M. Latest update on the Ro/SS-A autoantibody system. *Autoimmun Rev* **8**, 632-637 (2009).
37. Alspaugh, M. & Maddison, P. Resolution of the identity of certain antigen-antibody systems in systemic lupus erythematosus and Sjogren's syndrome: an interlaboratory collaboration. *Arthritis Rheum* **22**, 796-798 (1979).
38. Clark, G., Reichlin, M. & Tomasi, T.B., Jr. Characterization of a soluble cytoplasmic antigen reactive with sera from patients with systemic lupus erythmatosus. *J Immunol* **102**, 117-122 (1969).
39. Hung, T.*, et al.* The Ro60 autoantigen binds endogenous retroelements and regulates inflammatory gene expression. *Science* **350**, 455-459 (2015).
40. O'Donovan, A.*, et al.* Elevated risk for autoimmune disorders in iraq and afghanistan veterans with posttraumatic stress disorder. *Biol Psychiatry* **77**, 365-374 (2015).
41. Stein, M.B.*, et al.* Genome-wide Association Studies of Posttraumatic Stress Disorder in 2 Cohorts of US Army Soldiers. *JAMA Psychiatry* **73**, 695-704 (2016).
42. Eraly, S.A.*, et al.* Assessment of plasma C-reactive protein as a biomarker of posttraumatic stress disorder risk. *JAMA Psychiatry* **71**, 423-431 (2014).
43. Michopoulos, V.*, et al.* Association of CRP genetic variation and CRP level with elevated PTSD symptoms and physiological responses in a civilian population with high levels of trauma. *Am J Psychiatry* **172**, 353-362 (2015).
44. Smith, A.K.*, et al.* Differential immune system DNA methylation and cytokine regulation in post-traumatic stress disorder. *Am J Med Genet B Neuropsychiatr Genet* **156B**, 700-708 (2011).
45. Lindqvist, D.*, et al.* Proinflammatory milieu in combat-related PTSD is independent of depression and early life stress. *Brain Behav Immun* **42**, 81-88 (2014).
46. Louveau, A.*, et al.* Structural and functional features of central nervous system lymphatic vessels. *Nature* **523**, 337-341 (2015).
47. Derecki, N.C.*, et al.* Regulation of learning and memory by meningeal immunity: a key role for IL-4. *J Exp Med* **207**, 1067-1080 (2010).
48. Filiano, A.J.*, et al.* Unexpected role of interferon-gamma in regulating neuronal connectivity and social behaviour. *Nature* **535**, 425-429 (2016).
49. Kilaru, V.*, et al.* Genome-wide gene-based analysis suggests an association between Neuroligin 1 (NLGN1) and post-traumatic stress disorder. *Transl Psychiatry* **6**, e820 (2016).
50. Ashley-Koch, A.E.*, et al.* Genome-wide association study of posttraumatic stress disorder in a cohort of Iraq-Afghanistan era veterans. *J Affect Disord* **184**, 225-234 (2015).

51. Nievergelt, C.M.*, et al.* Genomic predictors of combat stress vulnerability and resilience in U.S. Marines: A genome-wide association study across multiple ancestries implicates PRTFDC1 as a potential PTSD gene. *Psychoneuroendocrinology* **51**, 459-471 (2015).
52. Almli, L.M.*, et al.* A genome-wide identified risk variant for PTSD is a methylation quantitative trait locus and confers decreased cortical activation to fearful faces. *Am J Med Genet B Neuropsychiatr Genet* **168B**, 327-336 (2015).
53. Logue, M.W.*, et al.* A genome-wide association study of post-traumatic stress disorder identifies the retinoid-related orphan receptor alpha (RORA) gene as a significant risk locus. *Mol Psychiatry* **18**, 937-942 (2013).
54. Xie, P.*, et al.* Genome-wide association study identifies new susceptibility loci for posttraumatic stress disorder. *Biol Psychiatry* **74**, 656-663 (2013).
55. Guffanti, G.*, et al.* Genome-wide association study implicates a novel RNA gene, the lincRNA AC068718.1, as a risk factor for post-traumatic stress disorder in women. *Psychoneuroendocrinology* **38**, 3029-3038 (2013).
56. Logue, M.W.*, et al.* The Psychiatric Genomics Consortium Posttraumatic Stress Disorder Workgroup: Posttraumatic Stress Disorder Enters the Age of Large-Scale Genomic Collaboration. *Neuropsychopharmacology* **40**, 2287-2297 (2015).
57. Rangaraju, S.*, et al.* Mood, stress and longevity: convergence on ANK3. *Mol Psychiatry* **21**, 1037-1049 (2016).
58. Papassotiropoulos, A. & de Quervain, D.J. Failed drug discovery in psychiatry: time for human genome-guided solutions. *Trends Cogn Sci* (2015).
59. Lang, P.J., Bradley, M.M. & Cuthbert, B.N. *International Affective Pictures System (IAPS): Affective Ratings of Pictures and Instruction Manual*, (University of Florida, Gainesville, Fl., 2008).
60. Wood, A.R.*, et al.* Defining the role of common variation in the genomic and biological architecture of adult human height. *Nat Genet* **46**, 1173-1186 (2014).
61. Locke, A.E.*, et al.* Genetic studies of body mass index yield new insights for obesity biology. *Nature* **518**, 197-206 (2015).
62. Heck, A.*, et al.* Genetic Analysis of Association Between Calcium Signaling and Hippocampal Activation, Memory Performance in the Young and Old, and Risk for Sporadic Alzheimer Disease. *JAMA Psychiatry* **72**, 1029-1036 (2015).
63. Heck, A.*, et al.* Converging genetic and functional brain imaging evidence links neuronal excitability to working memory, psychiatric disease, and brain activity. *Neuron* **81**, 1203-1213 (2014).
64. Hauer, D.*, et al.* Relationship of a common polymorphism of the glucocorticoid receptor gene to traumatic memories and posttraumatic stress disorder in patients after intensive care therapy. *Crit Care Med* **39**, 643-650 (2011).

65. Price, A.L., *et al.* Principal components analysis corrects for stratification in genome-wide association studies. *Nat Genet* **38**, 904-909 (2006).
66. Price, A.L., *et al.* Long-range LD can confound genome scans in admixed populations. *Am J Hum Genet* **83**, 132-135; author reply 135-139 (2008).
67. Sekhon, J.S. Multivariate and Propensity Score Matching Software with Automated Balance Optimization: The Matching Package for R. *J Stat Softw* **42**, 1-52 (2011).
68. Reisberg, D. & Heuer, F. Memory for emotional events. in *Memory and emotion* (eds. Reisberg, D. & Hertel, P.) 3-40 (Oxford University Press, 2004).
69. Li, H. & Durbin, R. Fast and accurate short read alignment with Burrows-Wheeler transform. *Bioinformatics* **25**, 1754-1760 (2009).
70. Quinlan, A.R. & Hall, I.M. BEDTools: a flexible suite of utilities for comparing genomic features. *Bioinformatics* **26**, 841-842 (2010).
71. McKenna, A., *et al.* The Genome Analysis Toolkit: a MapReduce framework for analyzing next-generation DNA sequencing data. *Genome Res* **20**, 1297-1303 (2010).
72. Van der Auwera, G.A., *et al.* From FastQ data to high confidence variant calls: the Genome Analysis Toolkit best practices pipeline. *Curr Protoc Bioinformatics* **43**, 11 10 11-33 (2013).
73. DePristo, M.A., *et al.* A framework for variation discovery and genotyping using next-generation DNA sequencing data. *Nat Genet* **43**, 491-498 (2011).
74. Guo, Y., Ye, F., Sheng, Q., Clark, T. & Samuels, D.C. Three-stage quality control strategies for DNA re-sequencing data. *Brief Bioinform* **15**, 879-889 (2014).
75. McKernan, K.J., *et al.* Sequence and structural variation in a human genome uncovered by short-read, massively parallel ligation sequencing using two-base encoding. *Genome Res* **19**, 1527-1541 (2009).
76. Schuster, S.C., *et al.* Complete Khoisan and Bantu genomes from southern Africa. *Nature* **463**, 943-947 (2010).
77. Cingolani, P., *et al.* A program for annotating and predicting the effects of single nucleotide polymorphisms, SnpEff: SNPs in the genome of Drosophila melanogaster strain w1118; iso-2; iso-3. *Fly (Austin)* **6**, 80-92 (2012).
78. Madsen, B.E. & Browning, S.R. A groupwise association test for rare mutations using a weighted sum statistic. *PLoS Genet* **5**, e1000384 (2009).
79. Price, A.L., *et al.* Pooled association tests for rare variants in exon-resequencing studies. *Am J Hum Genet* **86**, 832-838 (2010).
80. Lee, S., Abecasis, G.R., Boehnke, M. & Lin, X. Rare-variant association analysis: study designs and statistical tests. *Am J Hum Genet* **95**, 5-23 (2014).
81. Desikan, R.S., *et al.* An automated labeling system for subdividing the human cerebral cortex on MRI scans into gyral based regions of interest. *Neuroimage* **31**, 968-980 (2006).
82. Damasio, H. & Damasio, A.R. *Lesion Analysis in Neuropsychology*, (Oxford University Press, Oxford, 1989).

83. Ertl, V.*, et al.* Validation of a mental health assessment in an African conflict population. *Psychol Assess* **22**, 318-324 (2010).
84. Wilker, S.*, et al.* How to quantify exposure to traumatic stress? Reliability and predictive validity of measures for cumulative trauma exposure in a post-conflict population. *Eur J Psychotraumatol* **6**, 28306 (2015).
85. Onyut, L.P.*, et al.* Trauma, poverty and mental health among Somali and Rwandese refugees living in an African refugee settlement - an epidemiological study. *Confl Health* **3**, 6 (2009).
86. Kolassa, I.T., Kolassa, S., Ertl, V., Papassotiropoulos, A. & De Quervain, D.J. The risk of posttraumatic stress disorder after trauma depends on traumatic load and the catechol-o-methyltransferase Val(158)Met polymorphism. *Biol Psychiatry* **67**, 304-308 (2010).
87. Neuner, F.*, et al.* Psychological trauma and evidence for enhanced vulnerability for posttraumatic stress disorder through previous trauma among West Nile refugees. *BMC Psychiatry* **4**, 34 (2004).

Correspondence and requests for materials should be addressed to A.P. or A.H.

Acknowledgments

This work was funded by the University of Basel, the Swiss National Science Foundation (grants 163434, 147570, and 159740 to D.J.-F.d.Q. and A.P.), the European Community‘s Seventh Framework Programme (FP7/2007–2013) under grant agreement # 602450 (IMAGEMEND; grant to A.P and D.J.-F.d.Q.), the Novartis Foundation for medical-biological Research (grant #15C219 to A.P.), and by the German Research Foundation (Deutsche Forschungsgemeinschaft; grants to I.-T.K. and T.E.). The funders had no role in study design, data collection and analysis, decision to publish or preparation of the manuscript.

Contributions

A.P., D.J.F.d.Q., A.H., A.M. and M.F. conceived and designed the study. A.H., A.M., V.V., J.P., T.E., J.S., D.C., V.F., M.F., P.D., E.L., F.H., N.S., B.D.B., C.V., I.T.K., S.W., T.El., D.J.F.d.Q. and A.P. analysed the data. P.E., T.S., T.Sc. C.B. and N.B. provided bioinformatic support. A.P., A.H. and D.J.F.d.Q. wrote the manuscript. All collaborators reviewed and approved the final manuscript.

Competing interests

The authors declare no competing interests.

Table 1 Results of gene-based analyses in phenotypic extremes

Gene symbol	Gene name	Burden test *P*		Adaptive burden test *P*	
		nominal	adjusted¶	nominal	adjusted¶
TROVE2	TROVE Domain Family Member 2; Sjoegren Syndrome Type A Antigen; Ro60 KDa Autoantigen	2×10^{-6}	0.0004	4×10^{-5}	0.004
PKD2L2	Polycystin 2 Like 2, Transient Receptor Potential Cation Channel	0.00022	0.045	0.00288	0.317
CFAP57	Cilia And Flagella Associated Protein 57	0.00026	0.053	0.00035	0.038

¶: corrected for the number of genes reaching i-stat<0.001 in the respective test (burden test: 203 genes; adaptive burden test: 110 genes)

Table 2 Associations between common *TROVE2* SNPs and traumatic memory (P_{memory}), lifetime PTSD (P_{PTSD}), sex (P_{sex}), age (P_{age}), and number of traumatic event types (P_{events})

SNP ID	Localization	MAF	P_{sex}	P_{age}	P_{events}	P_{memory}	P_{PTSD}
rs6692342	upstream	0.25	0.868	0.952	0.712	0.007	0.0004
rs4657842	upstream	0.35	0.895	0.328	0.652	0.191	0.023
rs7554496	intronic	0.15	0.323	0.800	0.318	0.169	0.581
rs10801173	3'-UTR; intronic	0.47	0.235	0.316	0.746	0.186	0.024
rs41520747	downstream; intronic	0.18	0.360	0.669	0.791	0.587	0.017

Figure 1 Frequency histogram of aversive memory performance in 3418 healthy young adults. Dotted vertical blue and red lines at the right distribution tail represent the lower and upper, respectively, performance margins of subjects defined as high extremes. Dotted vertical blue and red lines at the left distribution tail represent the upper and lower, respectively, performance margins of subjects defined as low extremes.

Figure 2 Sequencing results of *TROVE2* (positions according to GRCh37/hg19 coordinates). Blue dots indicate variants with MAF ≤ 0.125 detected in the sample of 88 individuals with extreme aversive memory performance. Slash-separated numbers accompanying each dot indicate the frequency of occurrence of the respective minor allele in subjects with extremely high and extremely low performance (high/low). The minor allele of variant rs72740218 was observed in 10 high extremes and in 2 low extremes. The y-axis indicates –log10 of significance *P* of genetic association tests performed for each variant separately. For illustration purposes, two *TROVE 2* transcript variants (see also Fig. 4) are shown in the lower part of the figure. Blue filled rectangles represent coding exons, empty rectangles represent non-coding exons and UTRs.

Figure 3 *TROVE2* rs72740218 genotype-dependent differences in brain activity related to successful memory encoding of aversive stimuli as compared to neutral stimuli in 1258 healthy young subjects. Displayed are positive associations between genotype (number of minor *T* allele) and activity. The blue cross indicates the peak genotype-dependent activation (t = 5.80; P_{FWE} = 0.0003) in the left medial prefrontal cortex at (−5.5 38.5 36). Activations are overlaid on coronal, sagittal, and axial sections of brain images, displayed at t ≥ 3.1 ($P_{nominal}$ < 0.001) and using color-coded t values. L, left side of the brain; R, right side of the brain.

Figure 4 Association of *TROVE2* SNPs rs72740218 (A) and rs6692342 (B) in the human frontal cortex (data and boxplots retrieved from the BRAINEAC project server [23], http://www.braineac.org/, accessed on October 7, 2016). Panel A represents expression values of exon-specific probeset 2372955 (chr1:193053788-193053828). Panel B represents expression values of exon-specific probeset 2372928 (chr1:193028950-193029112; GRCh37/hg19 coordinates).

Figure 5 Schematic representation of selected *TROVE 2* RefSeq transcript variants (positions according to GRCh37/hg19 coordinates). UCSC identifiers are also given beneath each RefSeq identifier. Blue filled rectangles represent coding exons, empty rectangles represent non-coding exons and UTRs. SNPs rs6692342 and rs72740218 are zoomed in with 10 bases up- and downstream; +1: first coding base in first coding exon.

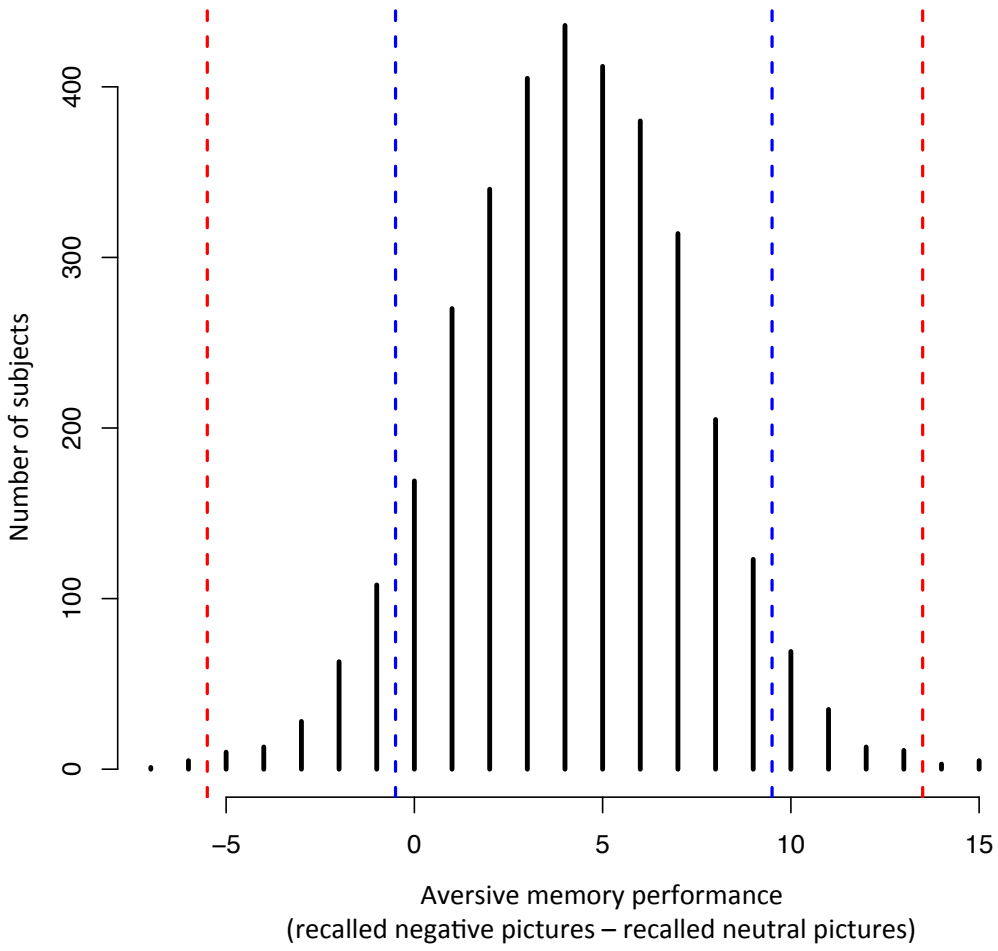
Number of subjects
0
100
200
300
400
–5
0
5
10
15
Aversive memory performance
(recalled negative pictures – recalled neutral pictures)

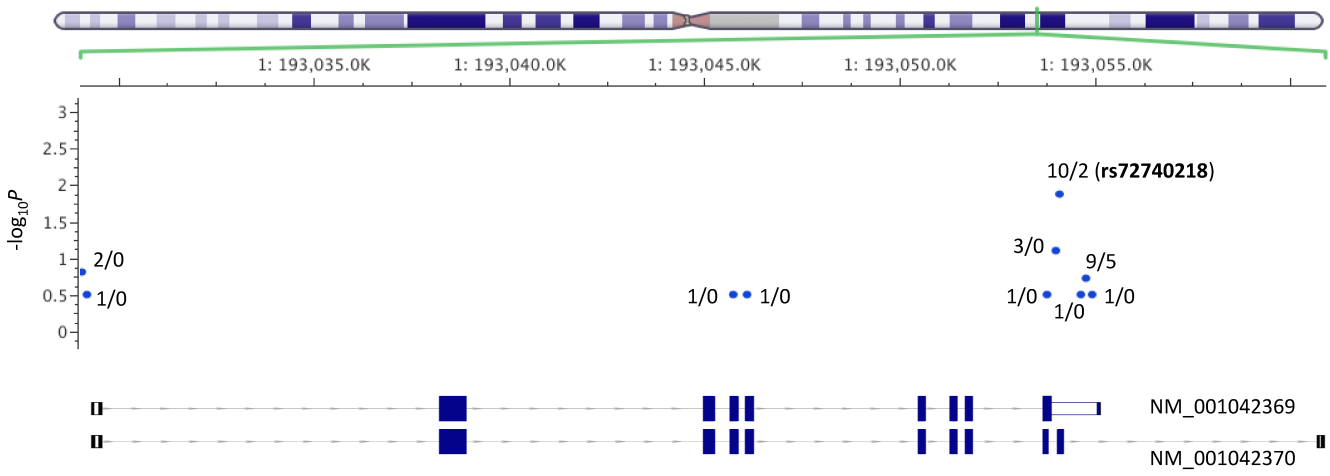
1: 193,035.0K
1: 193,040.0K
1: 193,045.0K
1: 193,050.0K
1: 193,055.0K
-log10P
3
2.5
2
1.5
1
0.5
0
10/2 (rs72740218)
3/0
9/5
2/0
1/0
1/0
1/0
1/0
1/0
1/0
NM_001042369
NM_001042370

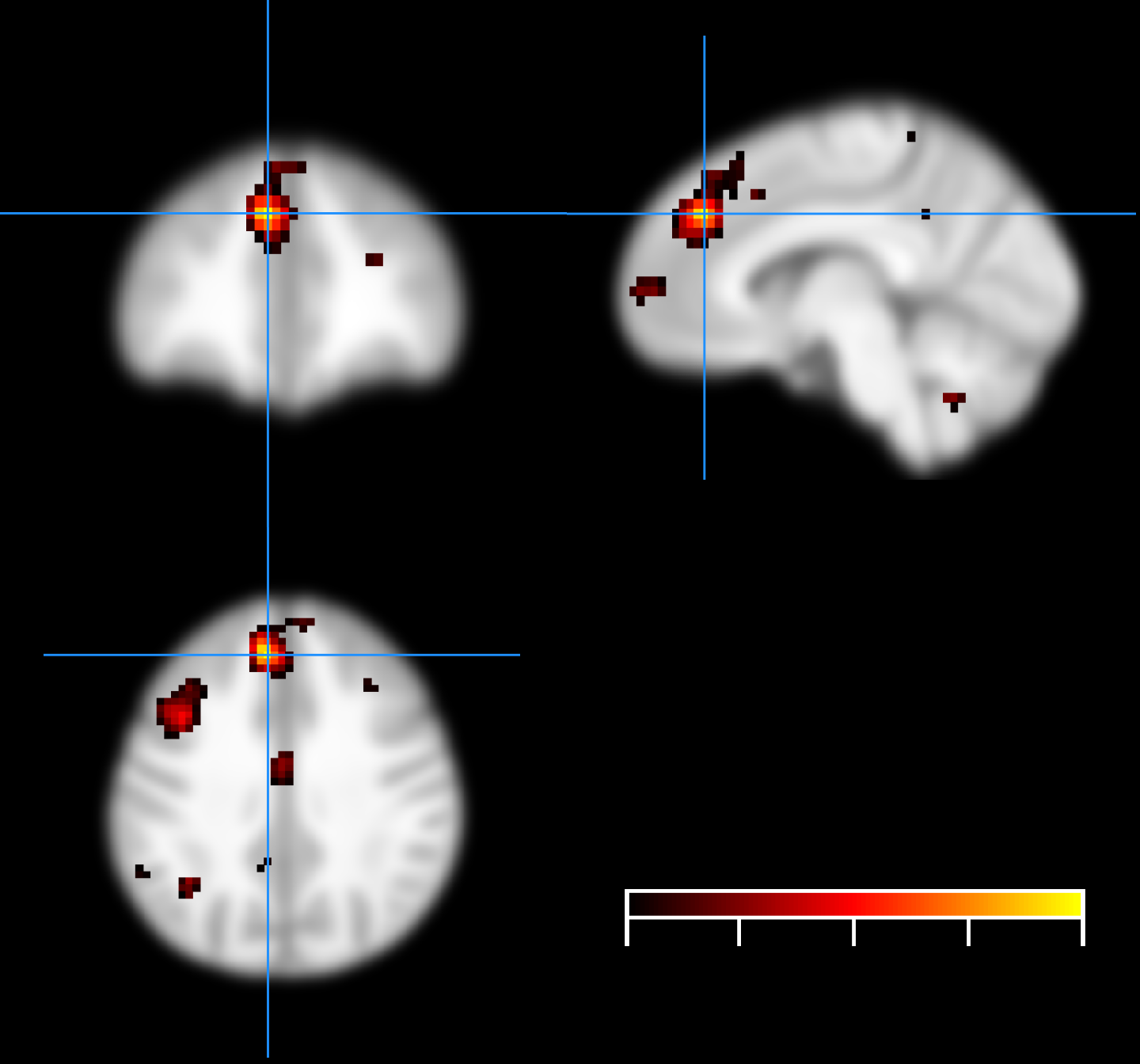

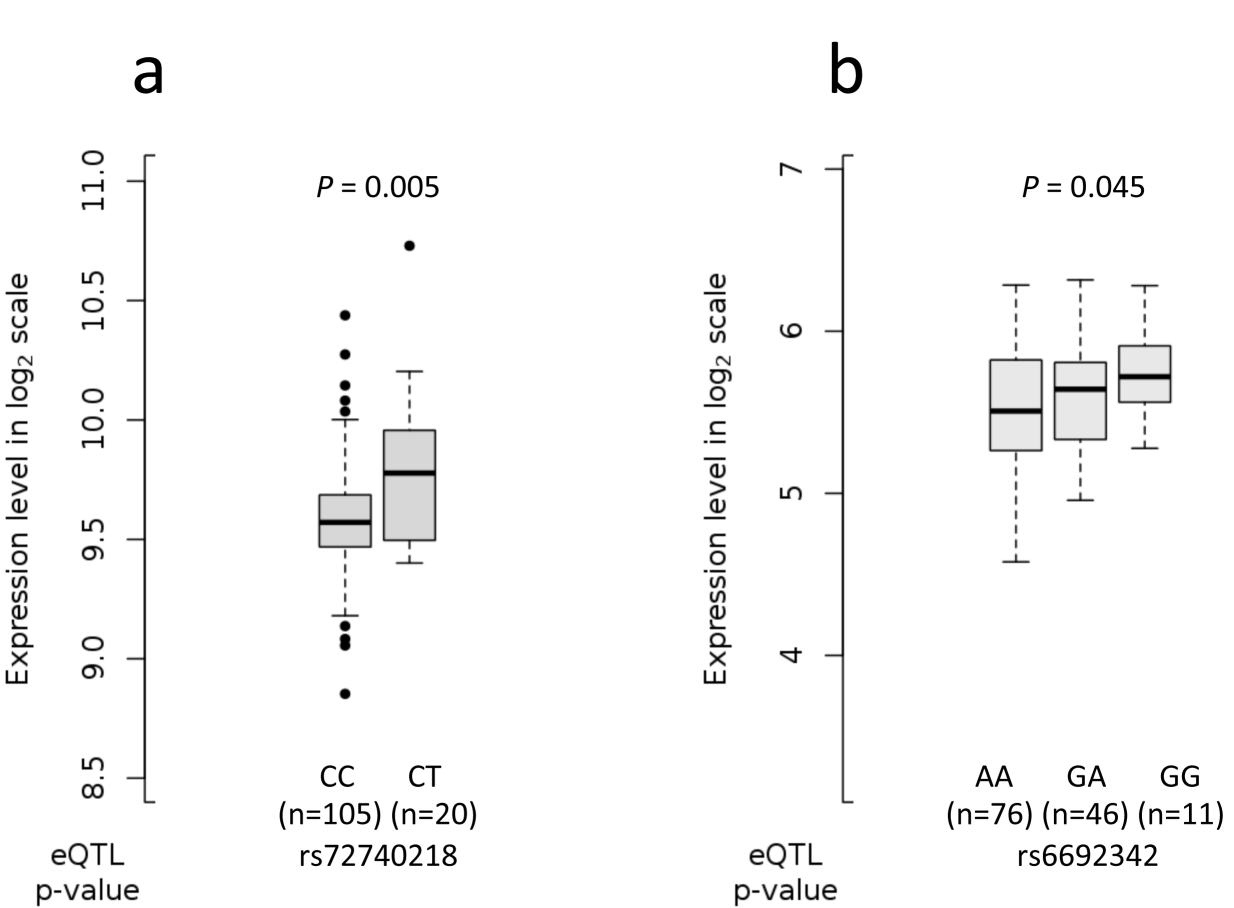
a
b
P = 0.005
P = 0.045
Expression level in log2 scale
8.5
9.0
9.5
10.0
10.5
11.0
4
5
6
7
CC
CT
(n=105)
(n=20)
AA
GA
GG
(n=76)
(n=46)
(n=11)
eQTL
p-value
rs72740218
eQTL
p-value
rs6692342

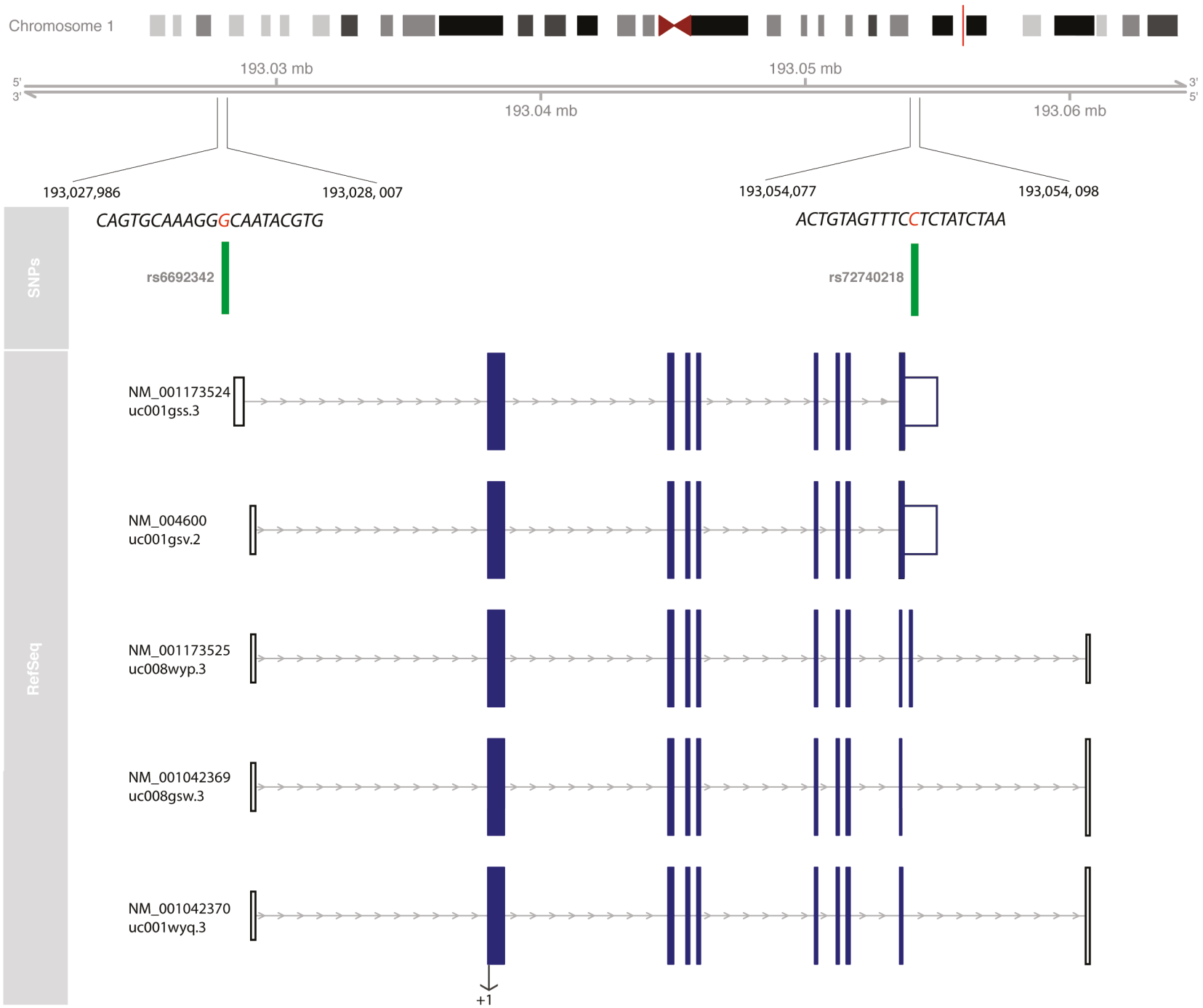
Chromosome 1
193.03 mb
193.05 mb
5'
3'
193.04 mb
193.06 mb
193,027,986
193,028, 007
193,054,077
193,054, 098
CAGTGCAAAGGGCAATACGTG
ACTGTAGTTTCCTCTATCTAA
SNPs
rs6692342
rs72740218
RefSeq
NM_001173524
uc001gss.3
NM_004600
uc001gsv.2
NM_001173525
uc008wyp.3
NM_001042369
uc008gsw.3
NM_001042370
uc001wyq.3
+1

Exome sequencing of healthy phenotypic extremes links *TROVE2* to emotional memory and PTSD

Angela Heck[1,2,3], Annette Milnik[1,2,3], Vanja Vukojevic[1,2,4], Jana Petrovska[1,2], Tobias Egli[1,2], Jochen Singer[5,6], Pablo Escobar[6,7,8], Thierry Sengstag[6,7,8], David Coynel[2,9], Virginie Freytag[1,2], Matthias Fastenrath[2,9], Philippe Demougin[1,2,4], Eva Loos[2,9], Francina Hartmann[1,2], Nathalie Schicktanz[2,9], Bernardo Delarue Bizzini[1,2,4], Christian Vogler[1,2,3], Iris-Tatjana Kolassa[10], Sarah Wilker[10], Thomas Elbert[11], Torsten Schwede[6,7,8], Christian Beisel[5], Niko Beerenwinkel[5,6], Dominique J.-F. de Quervain[2,3,9,+], Andreas Papassotiropoulos[1,2,3,4,*,+]

[1]Division of Molecular Neuroscience, Department of Psychology, University of Basel, CH-4055 Basel, Switzerland
[2]Transfaculty Research Platform Molecular and Cognitive Neurosciences, University of Basel, CH-4055 Basel, Switzerland
[3]Psychiatric University Clinics, University of Basel, CH-4055 Basel, Switzerland
[4]Department Biozentrum, Life Sciences Training Facility, University of Basel, CH-4056 Basel, Switzerland
[5]Department of Biosystems Science and Engineering, ETH Zurich, CH-4058 Basel, Switzerland
[6]SIB Swiss Institute of Bioinformatics, CH-4056 Basel, Switzerland
[7]Department Biozentrum, University of Basel, CH-4056 Basel, Switzerland
[8]sciCORE Center for Scientific Computing, University of Basel, CH-4056 Basel, Switzerland
[9]Division of Cognitive Neuroscience, Department of Psychology, University of Basel, CH-4055 Basel, Switzerland
[10]Clinical & Biological Psychology, Institute of Psychology & Education, Ulm University, D-89069 Ulm, Germany
[11]Department of Psychology, University of Konstanz, D-78457 Konstanz, Germany

*Correspondence to: andreas.papas@unibas.ch or angela.heck@unibas.ch
+ Co-senior author

Supplementary Table 1 Characteristics of the extreme phenotype groups and the whole sample

	High extremes	Low extremes	Significance *P* (extreme groups comparison)	Whole sample
Age, years (mean ± sd)	21.9 ± 2.9	22.4 ± 3.1	0.4	22.5 ± 3.5
Sex (% female)	43.2	43.2	1.0	64.6
HapMap, axis 1 (mean ± sd)	0.018 ± 0.001	0.018 ± 0.001	0.3	0.018 ± 0.001
HapMap, axis 2 (mean ± sd)	0.073 ± 0.002	0.074 ± 0.001	0.2	0.073 ± 0.002
MADRS (mean ± sd)	7.5 ± 5.8	6.8 ± 4.8	0.5	7.9 ± 5.9
STAI trait (mean ± sd)	33.8 ± 7.5	34.0 ± 6.9	0.9	37.1 ± 8.2
Episodic memory (mean ± sd)	32.0 ± 5.7	30.8 ± 9.6	0.5	29.4 ± 8.2
Aversive memory (mean ± sd)	**10.8 ± 0.8**	**-0.8 ± 0.8**	**1×10^{-73}**	4.2 ± 3.1
Negative pictures, free recall (mean ± sd)	15.4 ± 2.2	8.8 ± 3.5	3×10^{-17}	10.9 ± 3.3
Negative pictures, arousal (mean ± sd)	1.3 ± 0.4	1.2 ± 0.4	0.4	1.3 ± 0.3
Negative pictures, valence (mean ± sd)	-0.8 ± 0.2	-0.8 ± 0.2	0.5	-0.8 ± 0.2
Positive memory (mean ± sd)	7.4 ± 3.0	2.7 ± 2.5	1×10^{-11}	5.0 ± 3.1
Positive pictures, free recall (mean ± sd)	12.0 ± 2.8	12.4 ± 3.4	0.6	11.8 ± 3.5
Positive pictures, arousal (mean ± sd)	0.8 ± 0.5	1.0 ± 0.4	0.09	0.9 ± 0.4
Positive pictures, valence (mean ± sd)	0.8 ± 0.2	0.8 ± 0.2	0.6	0.8 ± 0.2
Neutral pictures, free recall (mean ± sd)	4.6 ± 2.1	9.6 ± 3.4	1×10^{-12}	6.7 ± 3.1
Neutral pictures, arousal (mean ± sd)	0.3 ± 0.3	0.3 ± 0.4	0.1	0.4 ± 0.3
Neutral pictures, valence (mean ± sd)	0.1 ± 0.1	0.1 ± 0.2	0.3	0.1 ± 0.2

Supplemetary Table 2 Top ten results of the Optimized Sequence Kernel Association Test (SKAT-O)

Gene symbol	Gene name	SKAT-O *P*
TROVE2	TROVE Domain Family Member 2; Sjoegren Syndrome Type A Antigen; Ro60 KDa Autoantigen	0.000215
GOSR1	Golgi SNAP Receptor Complex Member 1	0.000216
DHFRL1	Dihydrofolate Reductase Like 1	0.000249
CDH7	Cadherin 7	0.000373
TRPC1	Transient Receptor Potential Cation Channel Subfamily C Member 1	0.000426
MTUS2	Microtubule Associated Tumor Suppressor Candidate 2	0.000624
ABCC5	ATP Binding Cassette Subfamily C Member 5	0.000717
PLS1	Plastin 1	0.000742
WWP2	WW Domain Containing E3 Ubiquitin Protein Ligase 2	0.000818
KSR2	Kinase Suppressor Of Ras 2	0.000882

Supplementary Table 3 Non-sequenced extreme phenotype groups

	High extremes (N = 58)	Low extremes (N = 159)	Significance *P*
Age, years (mean ± sd)	21.7 ± 2.6	22.9 ± 3.9	0.027
Sex (% female)	67.2	77.4	0.1
HapMap, axis 1 (mean ± sd)	0.018 ± 0.001	0.018 ± 0.001	0.09
HapMap, axis 2 (mean ± sd)	0.073 ± 0.002	0.073 ± 0.001	0.5
Episodic memory (mean ± sd)	30.2 ± 6.6	30.1 ± 8.4	0.6 [$]
Aversive memory (mean ± sd)	10.7 ± 1.0	-2.0 ± 1.2	5×10^{-47} [$]

[$] denotes: age- and sex-corrected residuals were used for the calculation of *P* values

Supplementary Table 4 SNP effects on TROVE2 expression

exprID	chr	start	stop	$P_{frontal}$ rs72740218	$P_{frontal}$ rs6692342
2372927	chr1	193027785	193028845	0.025*	0.46
2372928^{Adj}	chr1	193028950	193029112	0.87	0.045*
2372937	chr1	193038268	193038643	0.081	0.55
2372942	chr1	193044968	193045143	0.72	0.5
2372944	chr1	193045645	193045763	0.56	0.85
2372945	chr1	193046043	193046134	0.78	0.76
2372947	chr1	193050506	193050594	0.89	0.59
2372952	chr1	193051316	193051415	0.61	0.96
2372953	chr1	193051699	193051824	0.28	0.92
2372955^{Adj}	chr1	193053788	193053828	0.0054*	0.56
2372957	chr1	193053865	193054077	0.031*	0.8
2372959	chr1	193054203	193054306	0.36	0.59
2372960	chr1	193054480	193055001	0.39	0.48
2372961	chr1	193055141	193055601	0.32	0.9
2372962	chr1	193056658	193056878	0.92	0.48
2372963	chr1	193059324	193060609	0.37	0.41
t2372924	chr1	193014651	193060891	0.41	0.94

exprID: exon-specific probeset ID based on Affymetrix's Human Exon 1.0 ST data. The exprID of the last row of this table is preceded by "t", which denotes transcript-level expression (i.e., Winsorised means over all exon-specific probesets). Exon-specific probeset ID's adjacent to rs72740218 and rs6692342 are marked with the superscript "Adj"; start, stop: chromosomal position of the probeset (positions according to GRCh37/hg19 coordinates); $P_{frontal}$ rs72740218: significance of association (additive genetic model) of SNP rs72740218 with probeset expression levels in the PFC. An asterisk "*" denotes nominally significant values; $P_{frontal}$ rs6692342: significance of association (additive genetic model) of SNP rs6692342 with probeset expression levels in the PFC. An asterisk "*" denotes nominally significant values.

Supplementary Table 5 Associations between specific events and *TROVE2* SNPs

	rs6692342	**rs4657842**	**rs7554496**	**rs10801173**	**rs41520747**
	P nominal	*P* nominal	*P* nominal	*P* nominal	*P* nominal
EVENT1	0.370	0.594	0.380	0.790	0.741
EVENT2	0.757	0.153	0.797	0.415	0.602
EVENT3*	0.532	0.224	0.038	0.260	0.092
EVENT4*	0.028	0.064	0.409	0.021	0.759
EVENT5	0.706	0.954	0.561	0.426	0.085
EVENT6	0.251	0.661	0.616	0.262	0.361
EVENT7	0.363	0.114	0.586	0.252	0.892
EVENT8	0.411	0.218	0.847	0.630	0.604
EVENT9	0.851	0.571	0.750	0.780	0.733
EVENT10	0.253	0.103	0.686	0.291	0.469
EVENT11	0.620	0.813	0.171	0.573	0.797
EVENT12	0.993	0.842	0.973	0.906	0.218
EVENT13	0.993	0.487	0.640	0.427	0.397
EVENT14	0.407	0.620	0.565	0.912	0.552
EVENT15	0.738	0.602	0.554	0.768	0.308
EVENT16	0.270	0.844	0.474	0.595	0.843
EVENT17	0.707	0.448	0.117	0.173	0.963
EVENT18*	0.057	0.008	0.395	0.081	0.137
EVENT19	0.412	0.974	0.933	0.755	0.816
EVENT20	0.193	0.347	0.091	0.671	0.690
EVENT21	0.408	0.320	0.816	0.651	0.225
EVENT22	0.453	0.554	0.060	0.821	0.593
EVENT23	0.861	0.287	0.267	0.629	0.654
EVENT24	0.665	0.218	0.966	0.619	0.211
EVENT25	0.935	0.735	0.437	0.623	0.639
EVENT26	0.249	0.316	0.107	0.097	0.533
EVENT27	0.381	0.886	0.165	0.887	0.877
EVENT28	0.656	0.775	0.661	0.274	0.413
EVENT29	0.103	0.276	0.302	0.408	0.664
EVENT30	0.325	0.553	0.394	0.213	0.992
EVENT31	0.167	0.206	0.068	0.103	0.661
EVENT32	0.725	0.303	0.418	0.918	0.329
EVENT33	0.728	0.791	0.118	0.649	0.976
EVENT34	0.643	0.491	0.394	0.676	0.665
EVENT35[$]	0.388	0.342	0.085	0.794	0.533
EVENT36[$]	0.388	0.342	0.085	0.794	0.533

EVENT1: Abduction; **EVENT2:** Serious accident; **EVENT3:** Violence by husband (only women); **EVENT4:** Severely beaten/tortured; **EVENT5:** Forced to marry as child; **EVENT6:** Fighting in combat; **EVENT7:** Bombing; **EVENT8:** Crossfire/snipers; **EVENT9:** Close to burning houses; **EVENT10:** Property confiscated; **EVENT11:** Dangerous evacuation; **EVENT12:** Injured by weapon; **EVENT13:** Circumcised by force (only women); **EVENT14:** Forced to be a prostitute or sexual slave (only women); **EVENT15:** Harassed by armed personnel; **EVENT16:** Imprisoned; **EVENT17:** Experienced poisoning or witchcraft; **EVENT18:** Raped; **EVENT19:** Intimate parts touched against will; **EVENT20:** Victim of robbery/looting; **EVENT21:** Offered sex for food or security (only women); **EVENT22:** Witnessed abduction/recruitment by force; **EVENT23:** Witnessed severe accident; **EVENT24:** Witnessed suicide; **EVENT25:** Witnessed mutilations/dead bodies; **EVENT26:** Witnessed beatings/torture; **EVENT27:** Close to combat situations; **EVENT28:** Witnessed forced circumcision; **EVENT29:** Witnessed forced prostitution/sexual slavery; **EVENT30:** Witnessed harassment by armed personnel; **EVENT31:** Witnessed severe injury by weapon; **EVENT32:** Witnessed killing/murder; **EVENT33:** Witnessed rape; **EVENT34:** Witnessed robbery/looting; **EVENT35:** Beaten by caretaker (e.g. parent, teacher, relatives); **EVENT36:** Burnt by caretaker

***** denotes: the frequency of this event was nominally associated with one or more *TROVE2* SNPs. **Note:** none of *TROVE2* SNPs was significantly associated with the frequency of any specific event after correction for multiple comparisons (36 tests performed); [$] denotes: low number of interviews for this event, limited validity of statistics.

Supplementary Table 6 Associations between common *TROVE2* SNPs and traumatic memory (P_{memory}) and lifetime PTSD, controlled for the occurrence of specific traumatic event types

SNP ID	P_{memory}	P_{PTSD}
rs6692342	0.009	0.0004
rs4657842	0.196	0.023
rs7554496	0.169	0.581
rs10801173	0.188	0.020
rs41520747	0.587	0.017

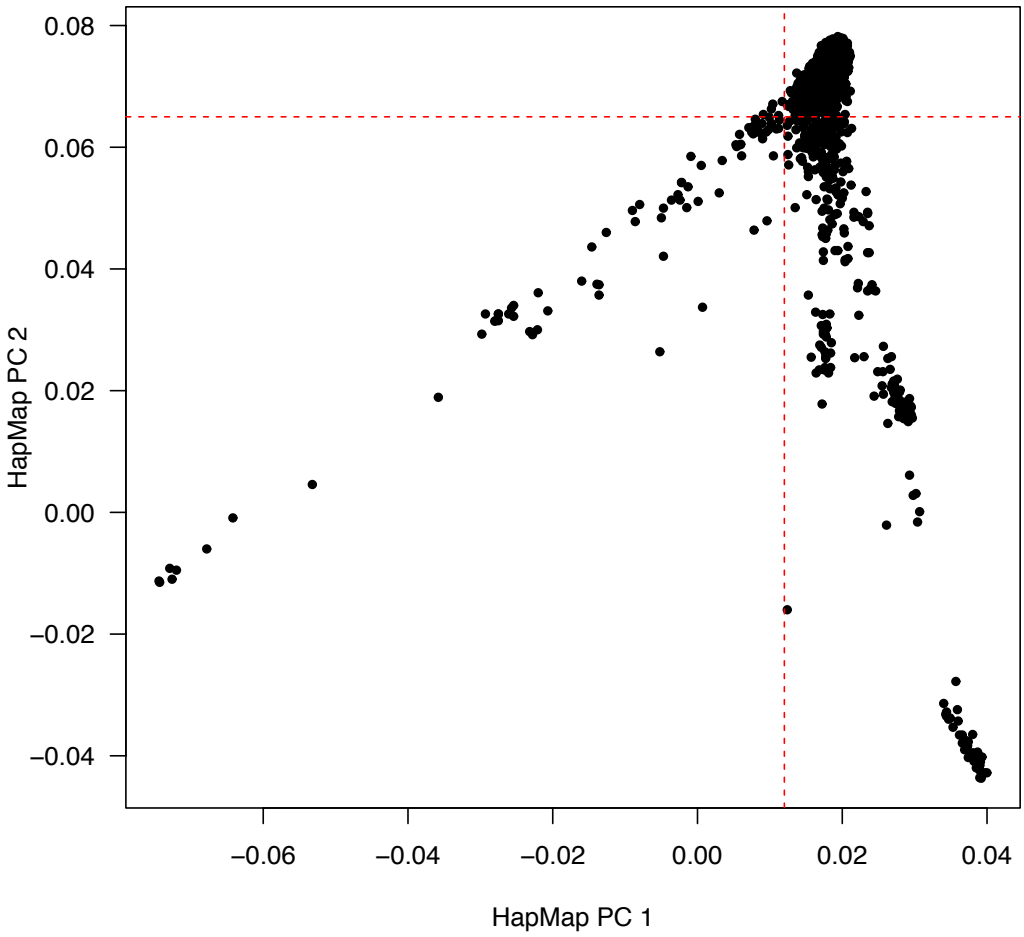

Supplementary Figure 1A Genetic data of 7 samples was projected onto the first two principal components of genetic variation in the HapMap3 reference sample, which consists of African, Asian and European samples. We included subjects with a broad European background (PC1 < 0.012 and PC2 < 0.065).

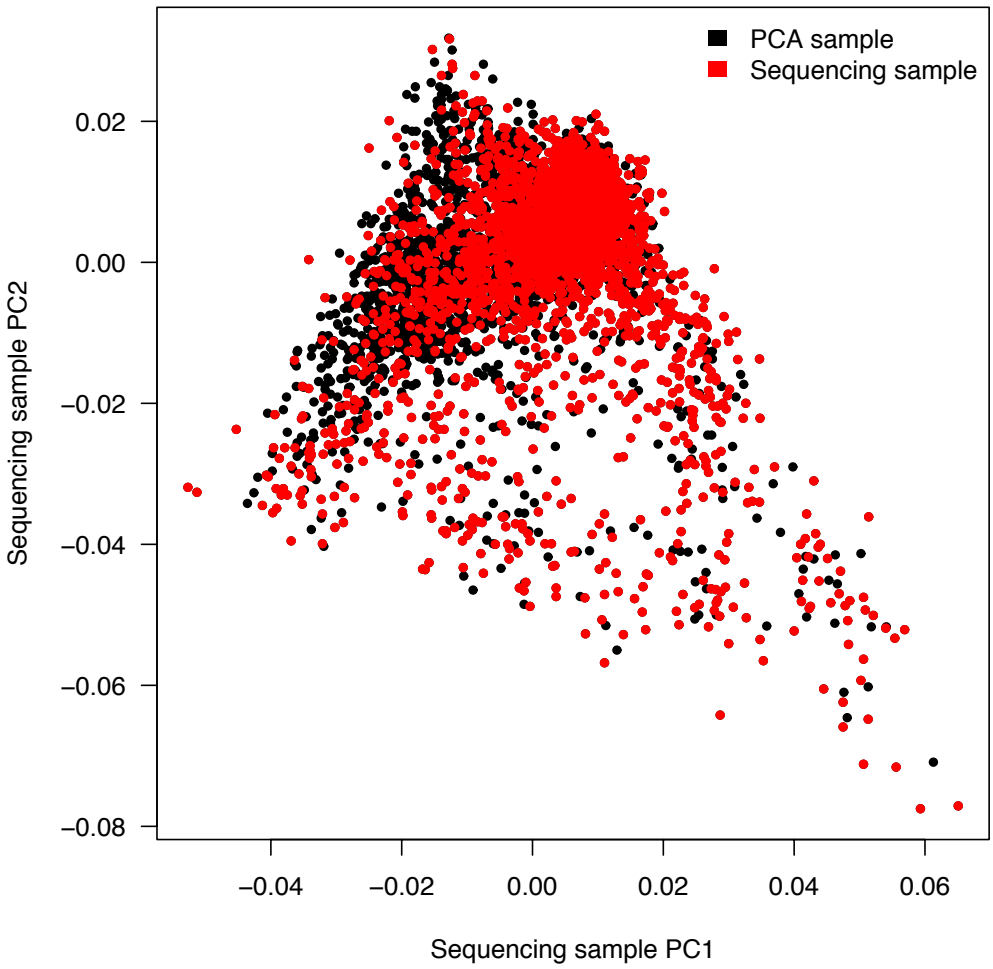

Supplementary Figure 1B Within the broad European sample, we performed PCA to derive the first two principal components as parameters for genetic similarity within European samples.

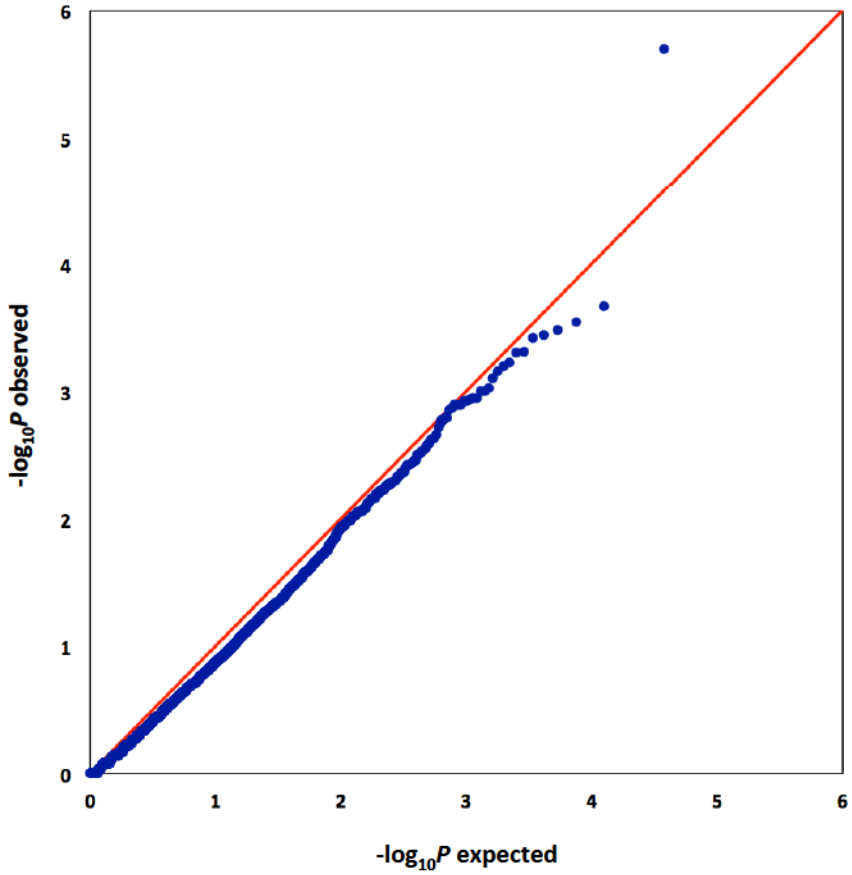

Supplementary Figure 2 QQ plot of the burden test.

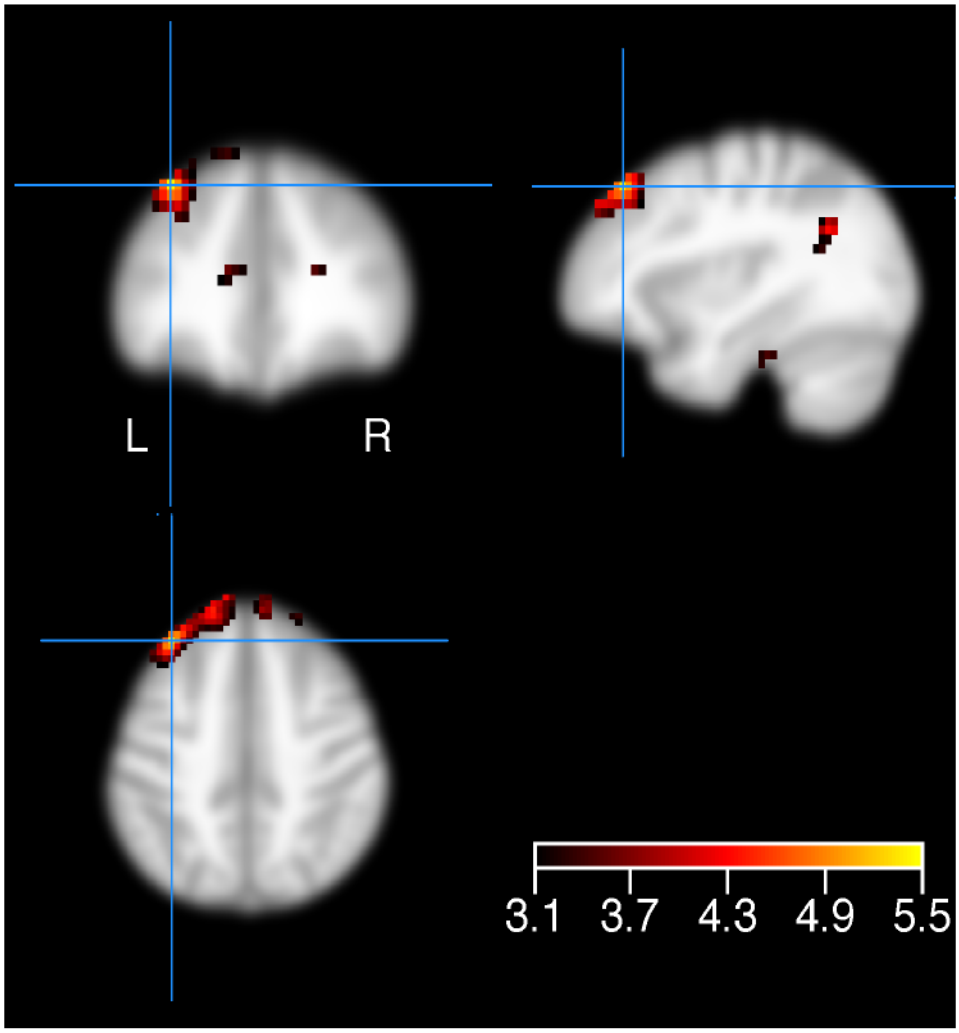

Supplementary Figure 3 *TROVE2* rs72740218 genotype-dependent differences in brain activity related to encoding of memory for negative information as compared to neutral information, independently of whether the information was later recalled or not. Displayed are gene dose-dependent (with increasing number of minor *T* allele) activity increases. The blue cross indicates the peak genotype-dependent activation (t = 5.39; P_{FWE} = 0.0015) in the left middle frontal gyrus at (−33, 36, 48). Activations are overlaid on coronal, sagittal, and axial sections of brain images, displayed at t ≥ 3.1 ($P_{nominal}$ < 0.001) and using color-coded t values. L, left side of the brain; R, right side of the brain.

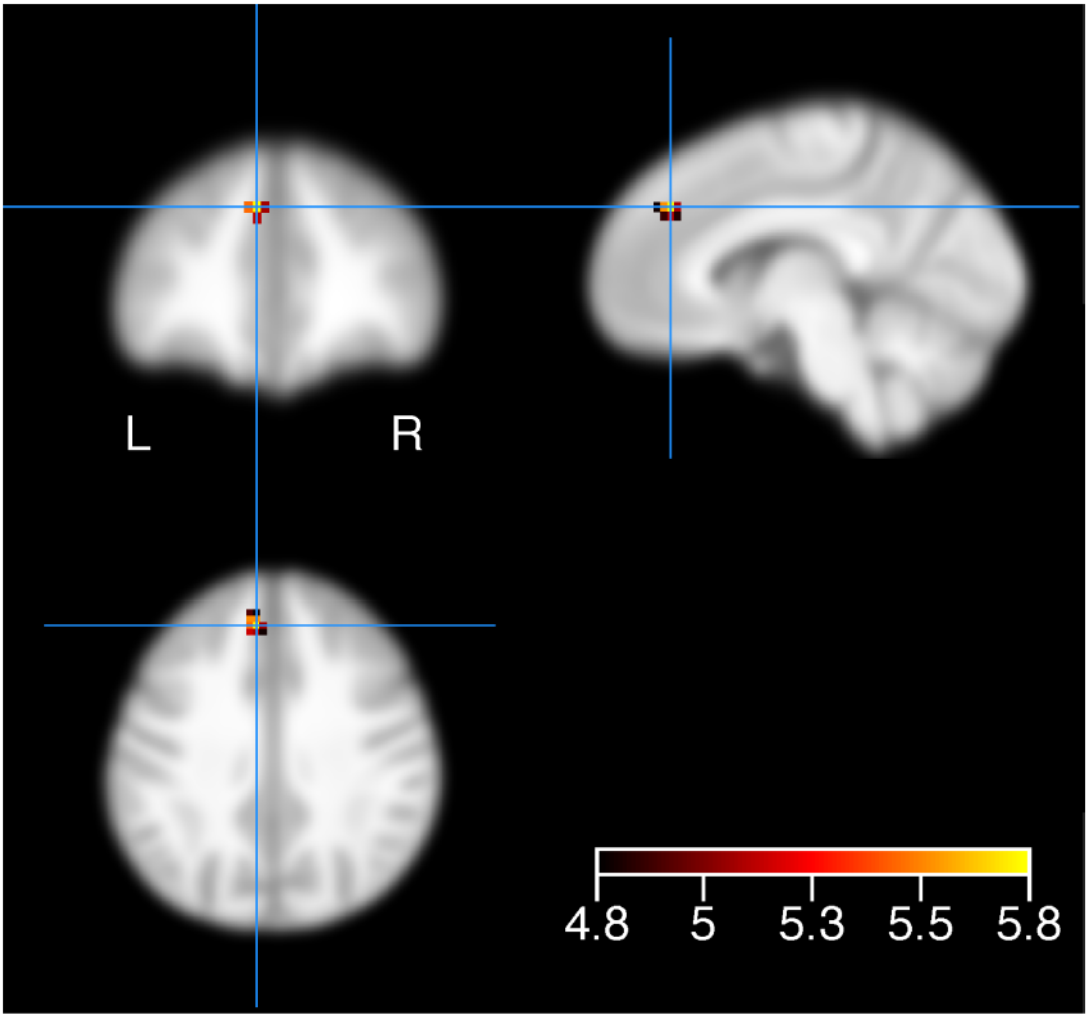

Supplementary Figure 4 *TROVE2* rs72740218 genotype-dependent differences in brain activity related to successful memory encoding of aversive stimuli as compared to neutral stimuli in 1258 healthy young subjects. Displayed are positive associations between genotype (number of minor *T* allele) and activity. The blue cross indicates the peak genotype-dependent activation (t = 5.80; P_{FWE} = 0.0003) in the left medial prefrontal cortex at (−5.5 38.5 36). Activations are overlaid on coronal, sagittal, and axial sections of brain images, displayed at t ≥ 4.81 (P_{FWE} < 0.05) and using color-coded t values. L, left side of the brain; R, right side of the brain.

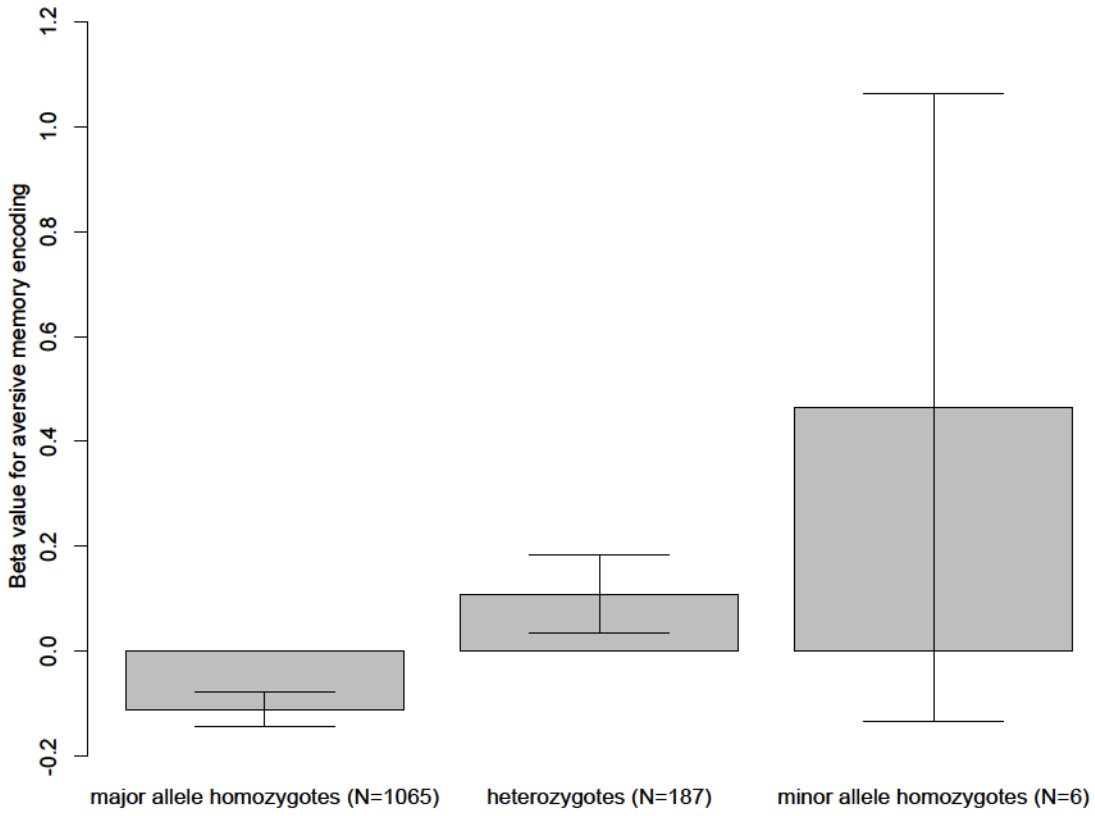

Supplementary Figure 5 *TROVE2* rs72740218 genotype-dependent differences in brain activity related to successful memory encoding of aversive stimuli as compared to neutral stimuli in 1258 healthy young subjects at coordinate position (-5.5., 38.5, 36). Error bars represent s.d.

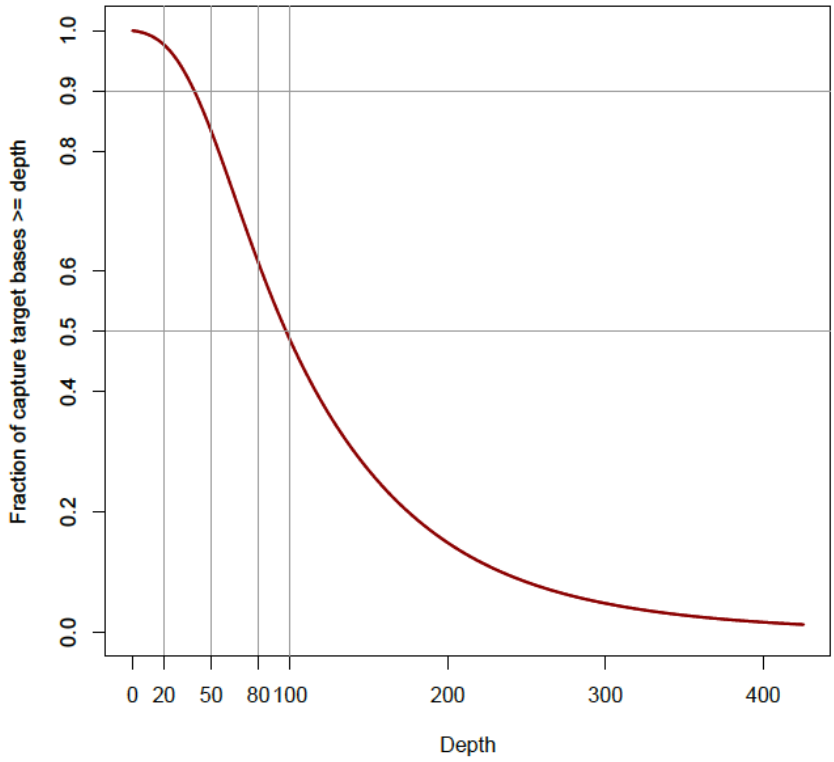

Supplementary Figure 6 Cumulative distribution of sequencing coverage observed among exome-targeted bases of sequenced individuals